

URTeC: 2876482

Characterizing Well Spacing, Well Stacking, and Well Completion Optimization in the Permian Basin: An Improved and Efficient Workflow Using Cloud-Based Computing

Piyush Pankaj, Schlumberger

Copyright 2018, Unconventional Resources Technology Conference (URTeC) DOI 10.15530/urtec-2018-2876482

This paper was prepared for presentation at the Unconventional Resources Technology Conference held in Houston, Texas, USA, 23-25 July 2018.

The URTeC Technical Program Committee accepted this presentation on the basis of information contained in an abstract submitted by the author(s). The contents of this paper have not been reviewed by URTeC and URTeC does not warrant the accuracy, reliability, or timeliness of any information herein. All information is the responsibility of, and, is subject to corrections by the author(s). Any person or entity that relies on any information obtained from this paper does so at their own risk. The information herein does not necessarily reflect any position of URTeC. Any reproduction, distribution, or storage of any part of this paper by anyone other than the author without the written consent of URTeC is prohibited.

Abstract

In a multiwell environment, the formula for improving the recovery efficiency per rock volume depends on the well spacing, stacking, and the completion strategy. Operators in the multi-benched Permian basin have been actively pursuing various trials of different combinations of vertical and horizontal spacing and completions of the wellbores. The study presented in this paper tries to achieve a prescription for successful exploitation of the cube of the unconventional reservoir rock through cloud-based multivariate simulation modeling.

A multilayer Wolfcamp earth model was calibrated. Reservoir characterization for petrophysical and geomechanical properties and discrete natural fracture network (DFN) were the fundamental steps to build the calibrated earth model. The tools used to derive the optimal solution space included over 500 multithreaded streamlined cloud-based complex hydraulic fracture simulations, use of unstructured gridding, fine-resolution numerical simulations, and finite-element geomechanical simulations. Optimal well landing was achieved by using a full-3D hydraulic fracture simulator. The effects of varying proppant-per-foot design (1,000 lbm/ft to 5,000 lbm/ft.); cluster spacing, stage spacing, and various well spacing (300 ft to 1,500 ft) configurations; and vertically stacked and staggered configurations are studied.

From the study, it is demonstrated that there are four elements that contribute to maximizing the recovery factor: optimal well landing, optimal well completion, optimal well spacing, and optimal time of completion. The parent-to-child relationship impairs production by up to 18% in 1 year, which is exemplified through finite-element simulations capturing the stress magnitude and direction reorientation. Stimulation sequences such as zippering and non-zippering the wellbores for completion were also found to be critical. Multiple sensitivities have therefore allowed us to define the envelope for optimal strategy of asset development in the reservoir volume.

With cloud computing serving as the enabler, the methodology discussed in the case study provides an integrated workflow to optimize the completion strategy in a multilayered unconventional formation such as in the Permian basin. The workflow helps to derive a structured approach to minimize the development cost, increase well completion effectiveness, and minimize the bypassed leftover hydrocarbon in the reservoir.

Introduction

A recent study done by Peacock et al. (2018) shows that Delaware -Midland basin has a maximum net present value (NPV) of designs with a proppant intensity of approximately 3000 lbm/ft (**Fig. 1**). Proppant intensity as of mid-2017 was reportedly 2,200 lbm/ft. Therefore, the bigger question is how do we improve the performance when we consider the spacing of multiple wellbores in a pad? Is performance driven by proppant intensity or are other factors such as cluster spacing, well spacing, stimulation sequence, and landing depths important, too? We will try to consider developing a holistic solution to answer these questions in this study.

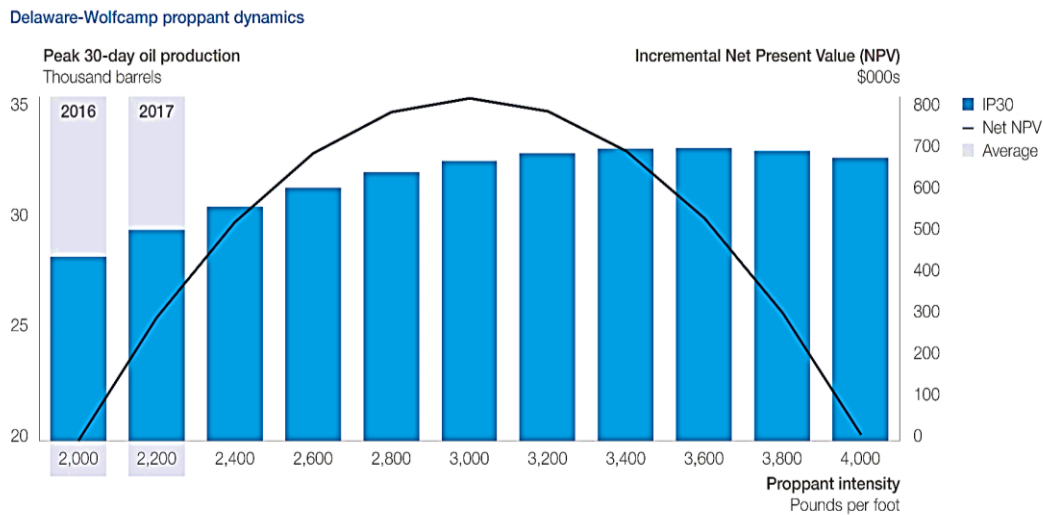


Fig. 1—Delaware-Wolfcamp wells are expected to reach an NPV maximum at a proppant intensity of 3,000 lbm/ft. (Peacock et al. 2018)

Economic exploitation of the unconventional reservoirs is largely dependent on overcoming the cost of operating an asset and drilling and completion of horizontal laterals with profitable production and recovery in the oil and gas market. In the current economic conditions and low oil and gas market prices, operators find it extremely difficult to gain positive swing in their balance sheets. One of the key opportunities presented by the challenging price environment to the geotechnical and petrotechnical community is to determine the most profitable recipe of well completion, spacing /stacking, and sequencing of fracturing on a multiwell pad system. Operators have been experimenting with various well completions by altering the number of stages, cluster spacing, fracture design, and pounds per foot of proppant on different configurations of well completions; among the experiments are vertical stacks on multiple benches; wine-racking, also commonly known as a chevron pattern (Fig. 2); and different horizontal well spacing.

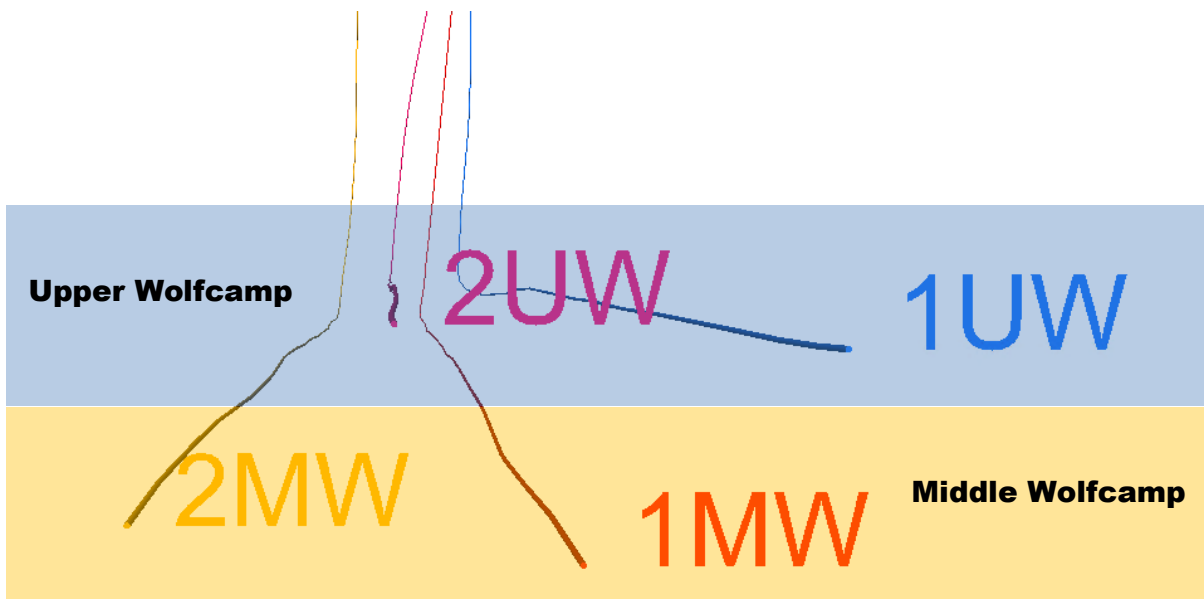


Fig. 2—Wells spaced in a wine-rack pattern in the upper and middle Wolfcamp.

These field experiments can be expensive and can lead to poor return on investment if incorrectly applied. The aim of this study is to provide a streamlined methodology in the modeling space for determining the best methods for exploiting such unconventional reservoirs. Such a methodology would help reduce the chances of failure on field and would help determine the true potential of the reservoir through optimizing well completion, well spacing, and well landing. Effective well completion and well spacing in an unconventional reservoir play is affected by reservoir heterogeneity, hydraulic fracture treatment volumes, dynamic reservoir and geomechanical changes, and consideration of development economics. The study produces a workflow that has been applied on the Wolfcamp asset of the Permian basin.

Background

The Wolfcamp shale (**Fig. 3**) covers most of the Midland Basin and ranges in thickness from 200 ft in the north of the basin to 2,600 ft in the south of the basin. The entire play is dominantly by a fine-grained, naturally fractured source rock (Collins et al. 2015). The depths of Wolfcamp formation range from 5,500 to 11,000 ft. The Wolfcamp is slightly overpressured, with the pressure gradient varying between 0.55 and 0.70 psi/ft. In the last few years, the Wolfcamp shale has become one of the most profitable and exploited unconventional oil plays in the United States. Almost all the operators are collecting a good share of their well inventory, which routinely yields over 1,000 BOPD initial production (IP) rates. The production declines within a short period (6 to 9 months). The recovery factors remain in the single digits for most of the operators. **Fig. 4** shows the location of Permian basin and a cross section showing the Delaware basin, central basin platform, Midland basin, and eastern shelf. The Wolfcamp, Spraberry, and Bone Spring are the most prolific formations in the basin. Parent-child well interaction has recently received a lot of discussion in literature for the Wolfcamp owing to multiple producing benches in the reservoir. These producing benches are commonly classified in four different layers, from top to bottom (Mohan et al. 2013): Wolfcamp A, Wolfcamp B, Wolfcamp C, and Wolfcamp D. Characteristics of the layers are as follows:

- Wolfcamp A is generally more carbonate rich than the other layers and can sometimes act as fracture containment layer. Some operators also refer to this as the Upper Wolfcamp and have further subdivided this into the Wolfcamp A1 and Wolfcamp A2 and, in some places, Wolfcamp A3.
- Wolfcamp B generally contains less carbonate and more quartz and tends to be highly organic rich. Some operators also refer to this as the Middle Wolfcamp and have further subdivided this into the Wolfcamp B1, Wolfcamp B2, and Wolfcamp B3.
- Wolfcamp C generally tends to have high clay content and is thick. Some operators also refer to this as the Lower Wolfcamp and have further subdivided this into the Wolfcamp C1 and Wolfcamp C2.
- Wolfcamp D generally tends to be the most geologically inconsistent zone across the Midland basin. Operators typically term this as the Cline shale, and where the Strawn formation is easily identified, operators classify this layer as the Wolfcamp D.

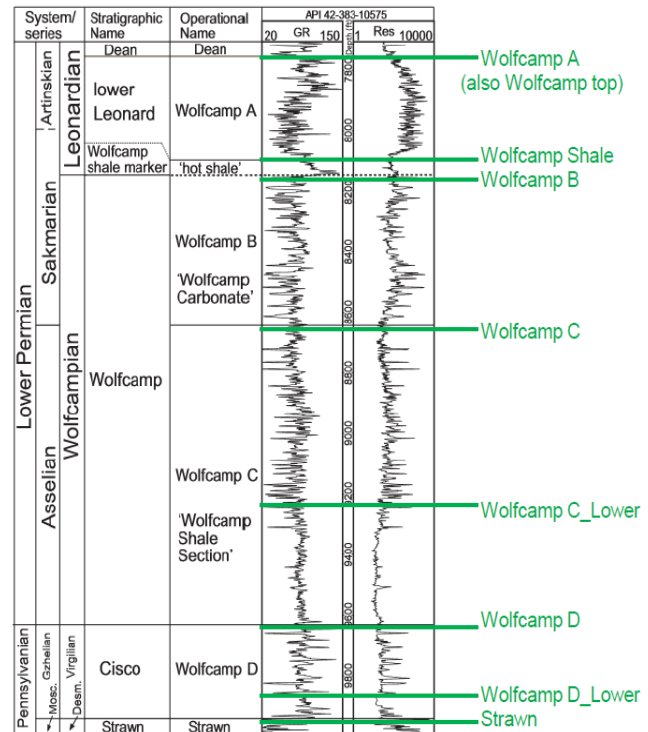


Fig. 3—Midland basin stratigraphy (Baumgardner et al. 2014).

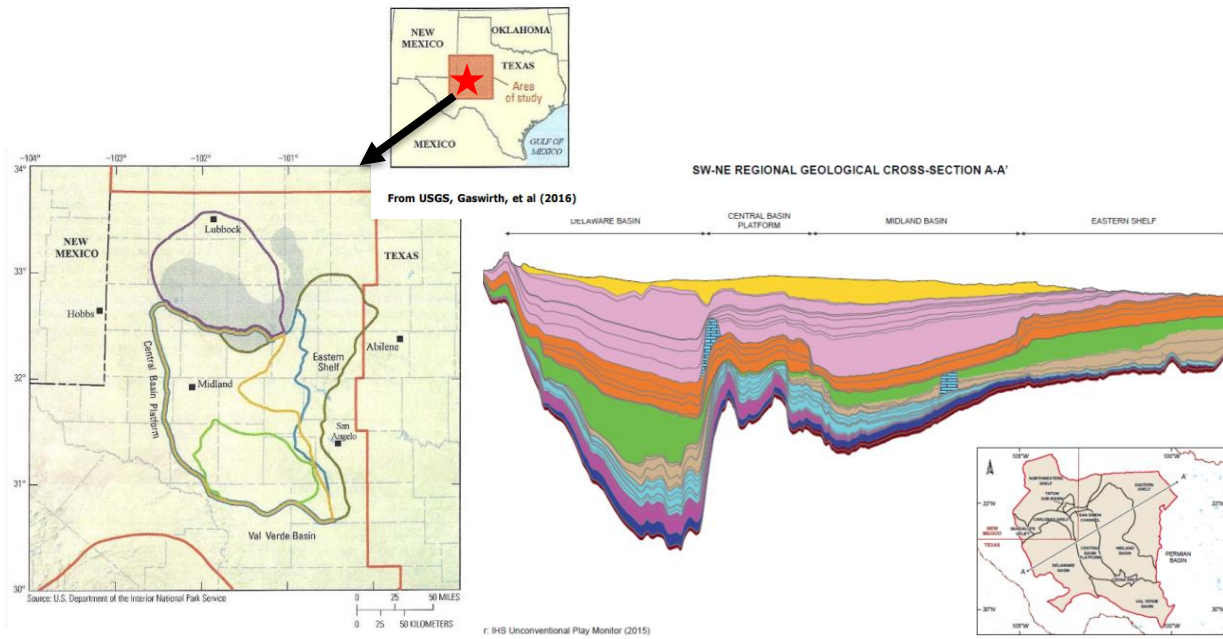


Fig. 4—Locations and stratigraphy. (a) Permian basin map from USGS (Gaswirth et al. 2016) (b) Taken from IHS unconventional play monitor, 2015, the cross section of the Permian basin showing Wolfcamp shale thickness and distribution across the basin.

Methodology

Hydraulic fracture and well completion optimization requires understanding of subsurface characteristics such as geology, petrophysics, and geomechanics and being able to predict the subsurface rock failure when extraneous fracturing fluid and proppant are pumped at high pressure from the surface. Although an exact presentation of hydraulic fracture geometry and its properties is extremely challenging, numerical simulation model combined with characterizing the rock properties can present the “near-equivalent” representation of the fracture geometry and its production response. Calibration data such as treating pressure history, net pressure matching, and microseismic data provide constraining dimensions to the nonunique solution of hydraulic fracture geometry representation.

In the methodology developed during the study presented in this paper, model calibration serves as crucial step during the process of asset optimization. The workflow for a multiwell pad where the wells are completed at the same time is depicted in **Fig. 5**, and the workflow for a multiwell pad where the wells are completed at different times is depicted in **Fig. 6**. **Fig. 6** adds steps to determine the geomechanical property changes while the parent well produces and depletes in time before the infill or child wells are stimulated. Numerous studies describing the hydraulic fracture reorientation on the child wells due to depletion on the parent have been published, for example, Marongiu-Porcu et al. (2015), Pankaj et al. (2016), Pankaj and Shukla (2018).

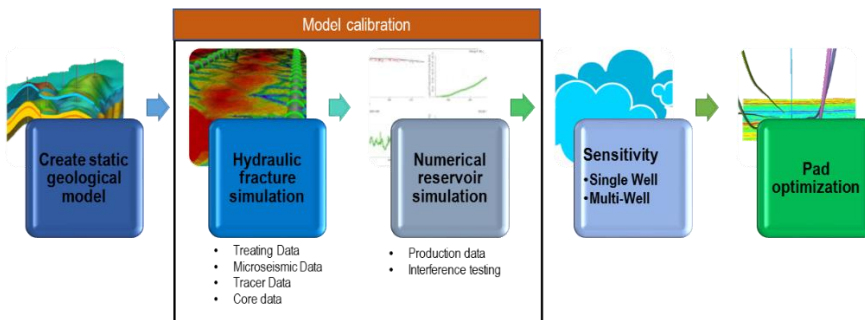


Fig. 5—Single or multiwell pad optimization workflow using multivariate sensitivity enabled through the cloud on a calibrated model where the wells are drilled and completed at the same time.

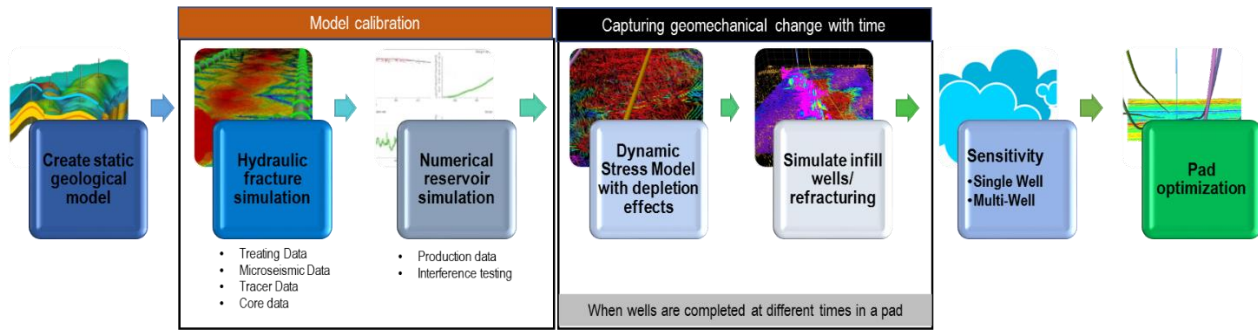


Fig. 6—Single or multiwell pad optimization workflow using multivariate sensitivity enabled through the cloud on a calibrated model where the wells are drilled and completed at the different times.

For this study, a small sector model was taken from the larger geological model in the area of interest (**Fig. 7**). The multiwell pad system comprised wells completed in the Upper Wolfcamp and wells completed in the Middle Wolfcamp shale formations. The first task was to determine the optimal completion design for these wells considering both cases—single-well and then multiple-well pad—for evaluating the impact of well spacing and stimulation sequencing such as zipper fracturing. Calibration of the model was done through matching the instantaneous shut-in pressure (ISIP) from the actual treatment data on the wells. Furthermore, the microseismic data were used to constrain the hydraulic fracture geometry. The natural fracture network in the Upper and Middle Wolfcamp shale was created using the borehole image logs and further propagated in the far field away from the wellbore using neural network and seismic attributes (**Fig. 8**).

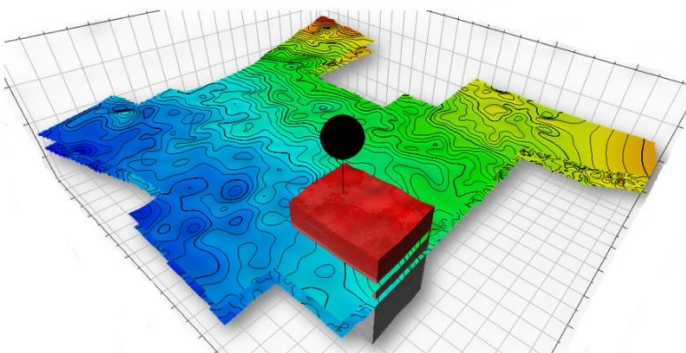


Fig. 7—Sector model cut out from bigger geological model for the study.

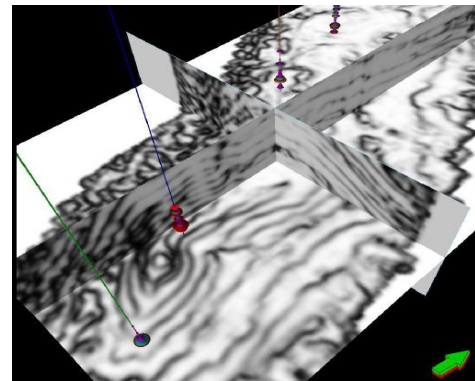


Fig. 8—Seismic attributes used to populate discrete natural fracture network.

The tools used for the study include a complex fracture model (Weng et al. 2011) that integrates the earth modeling and numerical reservoir simulation to the well completion design/analysis for unconventional reservoirs. The key processes include the construction of the geological model and detailed mechanical earth model (MEM) with the geomechanical and reservoir properties, completion description, simulation of fracturing treatment, calibration of the fracture model against microseismic observation, generation of the reservoir grid model, and production simulation. Works presented by Cipolla et al. (2011a) and Weng (2014) use this complete workflow or some of its components in reservoir characterization, completion design based on reservoir and completion quality, fracture simulation, calibration against microseismic, and production matching and simulation. The workflow used by the authors in aforementioned studies had been using manual simulations on selective scenarios, whereas the methodology presented in this paper explores a wider range of scenarios through sensitivity analysis performed by fracture and production models run in parallel in a cloud-based computing environment. Sensitivity analysis comprises numerical multivariate

analysis of various combinations of completion parameters forming a multidimensional chart to provide the optimal solution for completion and well spacing. The following parameters and their ranges are chosen to determine the resultant fracture geometries through the sensitivity on the parallel compute nodes:

- Proppant loading: 1,000 lbm/ft to 5,000lbm/ft
- Cluster spacing: 15 ft to 108 ft
- Number of stages: 25 to 167
- Horizontal well spacing: 300 ft to 1

The complex hydraulic fracture model was customized to be run in parallel outside of the desktop application. A separate orchestrator was created to extract the input model comprising the completion and production analysis settings on the calibrated model and to initiate the simulations of sensitivity on the parallel computing resource. The processes of fracture simulation, production gridding, and numerical simulations were all run on the compute nodes automatically without any manual intervention in a single batch process. The orchestrator was then able to retrieve the results of fracture and production simulation onto the desktop for analysis of the sensitivity cases.

Calibration of the Model

Model calibration comprises calibrating the hydraulic fracture model through matching the actual treating pressure data in the simulation model, matching the microseismic data footprint to the overall extent and azimuth of the fracture propagation, and. Finally. estimating the effective petrophysical properties such as porosity, permeability, and saturation of the rock and the fractured region. When available, other data such as tracer information, core data, and interference testing data may further help in improving the calibration of the hydraulic fracture and the geomodel. In the study, the geomodel was calibrated using the actual treatment data from pressure pumping (**Fig. 9**) and matching the footprint using the available microseismic data (**Fig. 10**) on the upper Wolfcamp wellbore. Fluid leakoff and end of the job ISIP were matched on a selective number of treatments chosen from heel, middle, and toe of the wellbore to expedite the process instead of matching the treatment data for each stage. Based on the calibration parameters from the three sections (heel, middle, and toe), the full wellbore simulation was run considering a pumping rate at 95 bbl/min with slickwater having ~ 1.5 cP fluid viscosity.

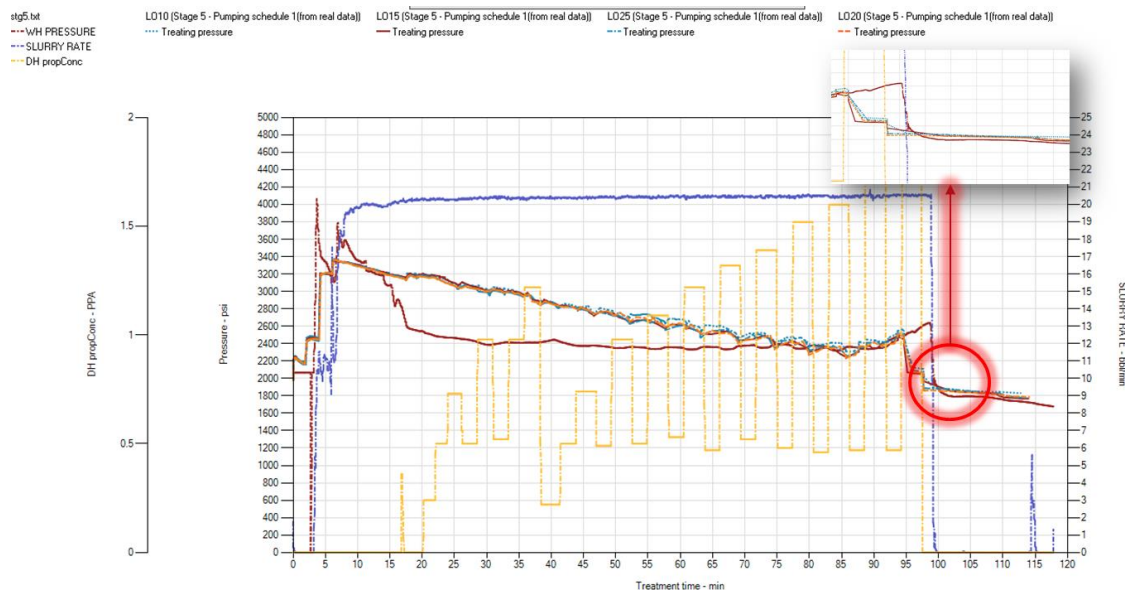


Fig. 9—Treating pressure match for calibrating hydraulic fractures matching the ISIP, fluid leakoff trend, and surface treating pressures.

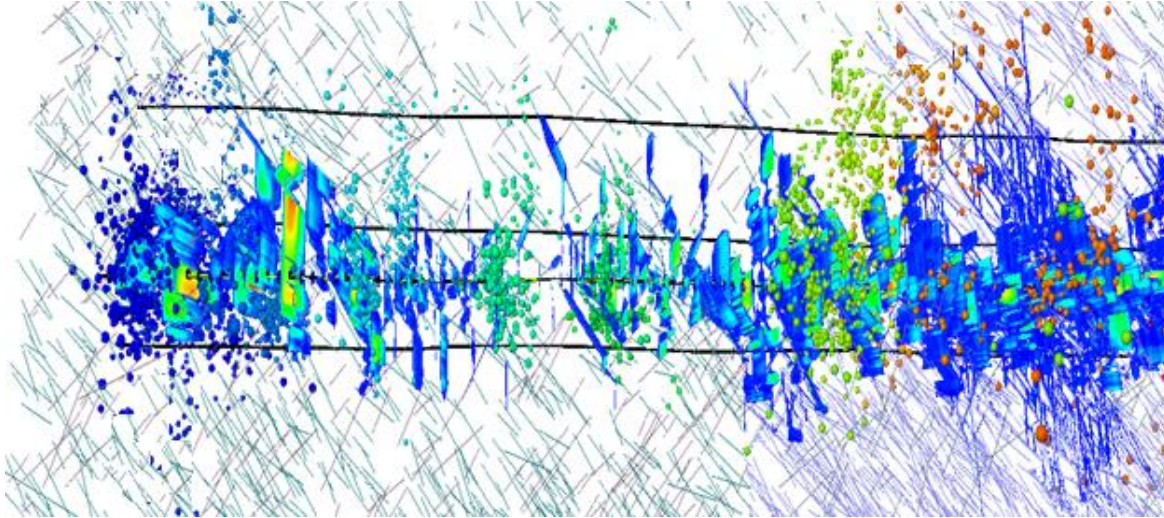


Fig. 10—Using available microseismic data to calibrate the fracture geometry by matching the footprint and fracture azimuth on some of the stages along the wellbore.

The objective of the sensitivity study was to determine the impact on fracture geometries and devise the most effective well completions. The recipe for appropriate and effective well completion depends hugely on the geological and geomechanical properties of the formation. Therefore, the results arising from the methodology presented here should not be applied to all the well locations in the Wolfcamp. Systematic and consistent approach as outlined above in the workflow can however help to narrow down the uncertainty for solving the puzzle around asset optimization.

Well Completion Optimization

After calibration of the Upper Wolfcamp wellbore, sensitivity cases were run in the cloud to derive the following six parameters of hydraulic fractures averaged for the full wellbore for the single-well scenario and the multiwell scenario having wells in upper and middle Wolfcamp.

1. Surface area, propped and total
2. Net pressure in the fracture at the end of treatment
3. Fracture height, propped and total
4. Average fracture width
5. Average fracture length
6. Average conductivity

Additionally, the impact on fracture geometries for the horizontal wells in the upper Wolfcamp were studied for zipper and non-zipper stimulation sequence. Further, production simulation based on numerical reservoir simulation engines were also made on selective cases.

Results

Single-Well Scenario

Variation with Proppant Loading

Proppant loading is directly correlatable to economics because it costs more to pump more. Therefore, balancing the productivity of the wellbore with the cost of treatment is extremely important, especially in the cost-sensitive pricing environment of today. We therefore explore the improved fracture geometry resulting from varying the proppant loading in the treatment job while keeping the other completion parameters such as cluster spacing, number of stages, number of clusters, and the fracturing fluid type fixed to the base case.

It is generally observed that the wells would perform better in terms of production when bigger treatment jobs with higher proppant volume are pumped on the wellbore because the total surface area trend as shown in **Fig. 11** improves with increasing volume of proppants in the pump schedule. However, the propped surface area shows an early

plateauing trend due to the limited capacity of the high density and transporting into the height and the far tips across the narrow channels of the hydraulic fractures. The hydraulic fracture complexity due to the presence of natural fractures may create bigger fracture volume but restricts the high concentration of proppants to turn across the bends. Hence, the proppant loading beyond 3000 lbm/ft does not show much additional improvement in the propped surface area. The propped surface area ratio to the total surface area therefore drops from 70% at 1000 lbm/ft to 50% at 5000lbm/ft.

Fig. 12 shows the increasing trend of net pressures as higher proppant loading is being pumped on the treatment. Net pressure is defined as the pressure in the fracture minus the in-situ stress. Also, it is noticed that from the field experiences in the Wolfcamp, achieving over 500 psia of net pressure becomes extremely challenging because the risk of screening out the hydraulic fractures increases.

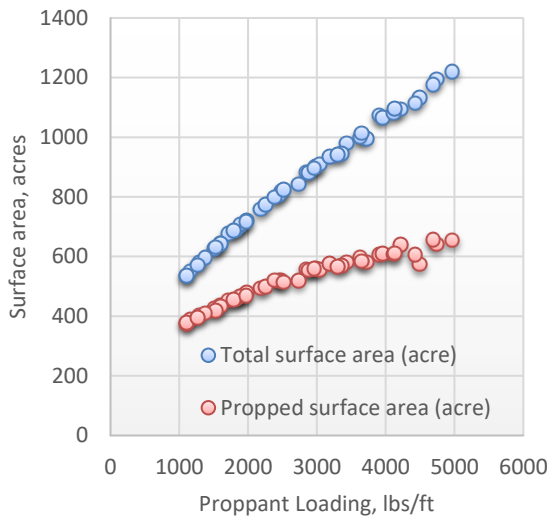


Fig. 11—Surface area with proppant loading,

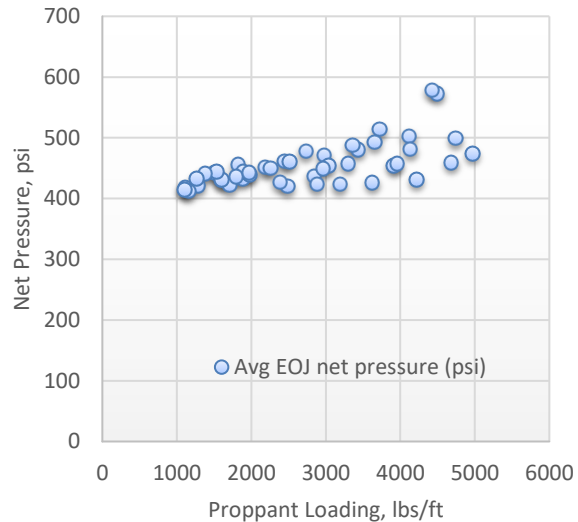


Fig. 12—Average net pressure with proppant loading.

The hydraulic fracture height as seen in **Fig. 13** shows that lower concentration of proppants in the hydraulic fractures at lower pounds per foot is much more easily carried in height at the 95 bbl/min pump rate than at the higher concentration.

With increasing concentrations of proppants being pumped at higher loadings, the average fracture width, as seen in **Fig. 14**.

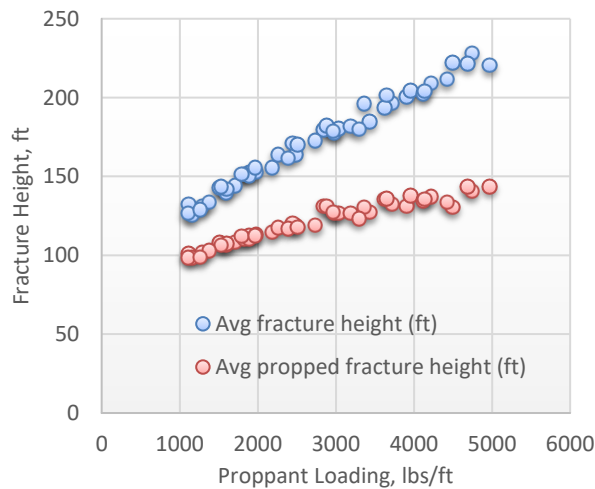


Fig. 13—Average fracture height with proppant loading.

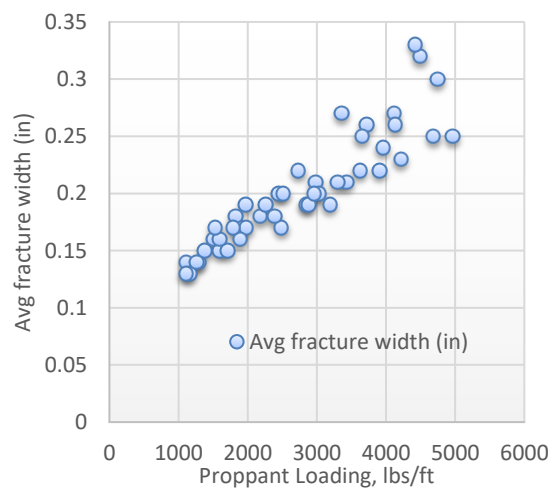


Fig. 14—Average fracture width with proppant loading.

Fig. 15 presents the variation of the average fracture extent/fracture length in the direction of maximum horizontal stress. It is seen that since the pad creates most of the fracture length upfront, the increasing amount of proppants coming after the pad can only help the length extension marginally and stretch the footprint by 9% when jobs are pumped at 5000 lbm/ft. as against 1000 lbm/ft.

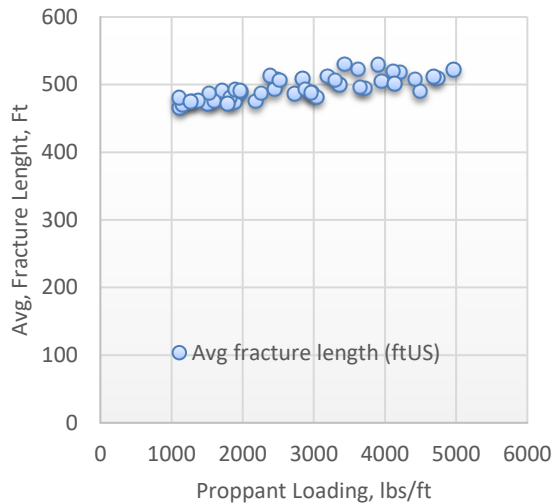


Fig. 15—Average fracture length with proppant loading.

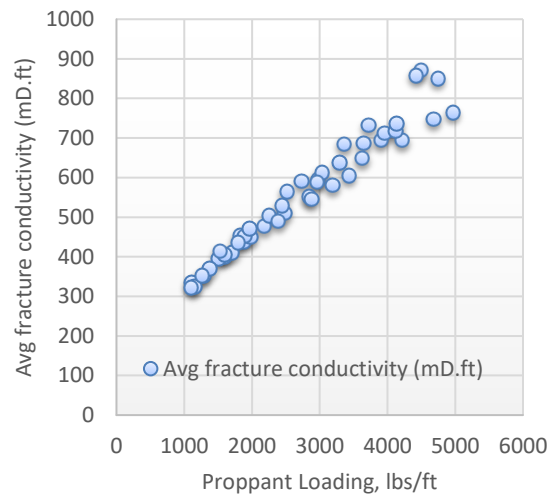


Fig. 16—Average fracture conductivity with proppant loading.

The average conductivity is a function of fracture width and the fracture permeability and is represented in **Fig. 16**. It is expected that as more proppant is pumped, the higher concentration of proppants in the hydraulic fracture improves the fracture permeability and the width, as seen in Fig. 14. It is noticeable that the range of fracture conductivity is significantly large because the conductivity increases over 250% when the proppant loading is increased from 1,000 lbm/ft. to 5,000 lbm/ft.

Cluster Spacing

In the Wolfcamp, one of the biggest challenges for operators is to determine the right cluster spacing in context of the specific well completion and well spacing. Operators have seen field responses to reduced cluster spacing tests on well's productivity. As we explore the impact of cluster spacing, we kept the proppant loading constant to the base case of 1,100 lbm/ft and the same fracturing fluid.

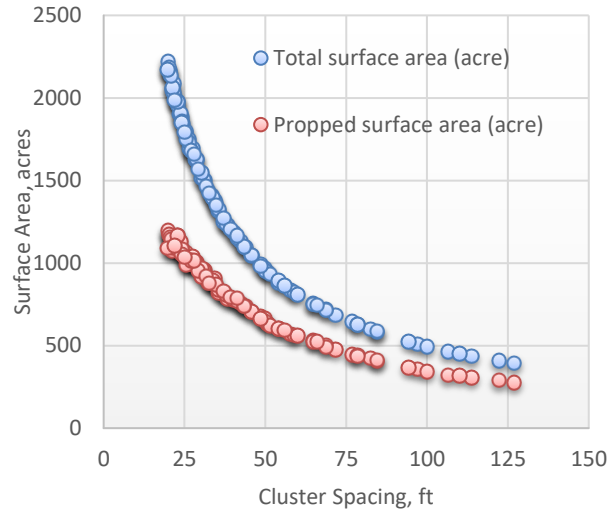


Fig. 17—Surface area with cluster spacing.

Fig. 17 shows that as the cluster spacing is reduced, the surface area also improves considerably. This is due to the fact that as the cluster spacing is reduced, we see more near-wellbore complexity as the fracturing fluid interacts with the natural fractures. Smaller cluster spacing would therefore help to create a denser fracture geometry concentric around the wellbore as when compared to the longer cluster spacing that would have more chances to grow in extent (**Fig. 18**).



Fig. 18—Heat map of hydraulic fractures in a gun-barrel view (red color with higher intensity represents more fracture counts and blue color shows lower fracture count). (a) More dense and shorter fracture extent with a shorter cluster spacing completion system, and (b) longer fracture length with relatively lesser density of hydraulic fractures in the near-wellbore region in a longer cluster spacing system.

Fig. 19 shows that the average net pressure developed in the fracture increases as the clusters are spaced closely. It is seen that in the base completion with three clusters per stage, the cluster spacing below 20 ft increases the net pressure generation beyond 1,000 psi, which becomes extremely difficult to attain in practical pumping. As the fracture initiation points in the wellbore become closer with smaller cluster spacing, there is considerable increase in the stress shadow amongst the clusters. Hence, at such extremely low cluster spacing, some of the cluster would choke during the pumping and only a few other clusters will preferentially take the fracturing fluid. Hence, when planning for smaller cluster spacing, increasing the number of clusters per stage becomes extremely important to improve the chances of pumping the designed treatment volume in the reservoir and avoid screening out the proppants in the wellbore.

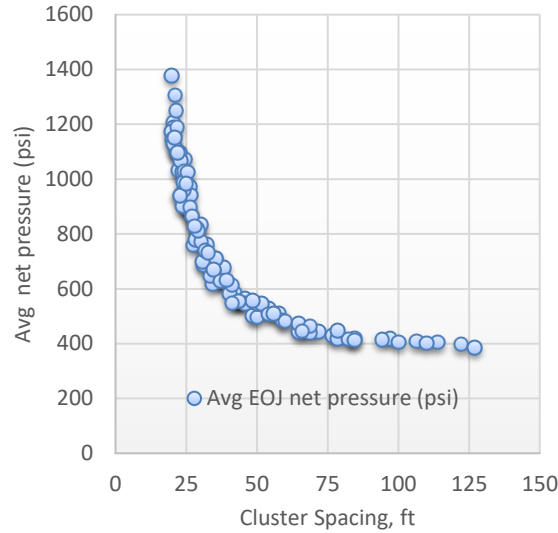


Fig. 19—Average net pressure with cluster spacing.

It is also interesting that as the clusters are brought closer, the average fracture height shows a minor increase (**Fig. 20**), and this is attributed to the increasing stress shadow between the initiating fracture fronts. The stress shadow effect compresses and pushes the fracture propagation front towards height since the competition and proximity in the horizontal direction of propagation increases at short cluster spacing.

The propped height, on the other hand (**Fig. 18**), shows a slightly increasing trend with the decreasing cluster spacing until approximately 30-ft cluster spacing. The propped height stays almost constant as the cluster spacing tightens beyond 30 ft.

The average fracture width computed for the full fracture systems across all the stages shows an increasing trend with reduced cluster spacing (**Fig. 21**). This is attributed to the fact that the net pressure shows significant increase as the fractures are brought closer together with shorter cluster spacing and the fracture width is proportional to the net pressure generated in the fracture.

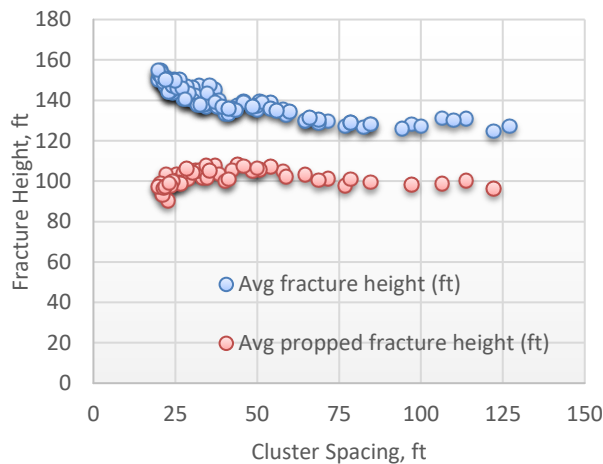


Fig. 20—Average fracture height with cluster spacing.

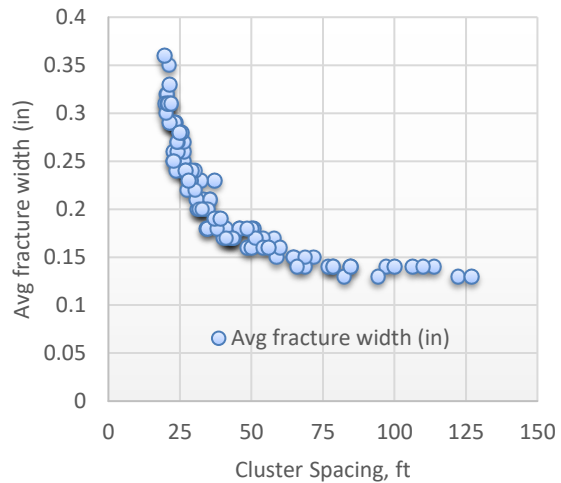


Fig. 21—Average fracture width with cluster spacing.

As the clusters are brought closer, the fracture geometry is more centered in the near-wellbore area and hence the lengths are shorter, as seen in **Fig. 22**. The hydraulic fracture lengths are almost 1.5 times more when we compare the 30-ft cluster spacing to a 100-ft cluster spacing scenario. Therefore, although this might not be very important when

considering a single-well scenario, in a multiwell system, the horizontal well spacing would be impacted by the completion’s cluster spacing as well. Fracture conductivity follows the trend of the fracture width (**Fig. 23**).

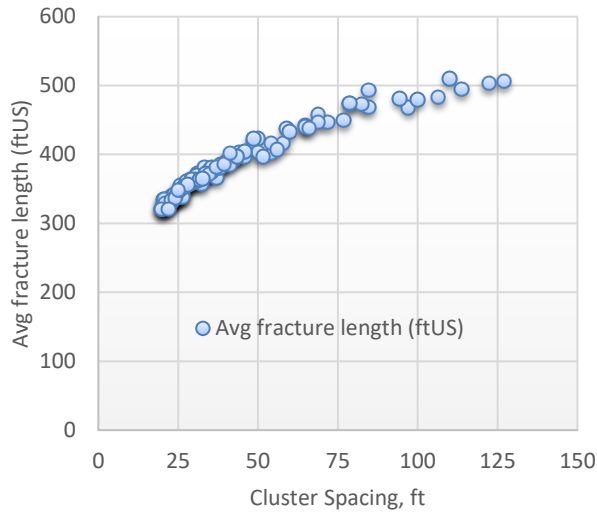


Fig. 22—Average fracture length with cluster spacing.

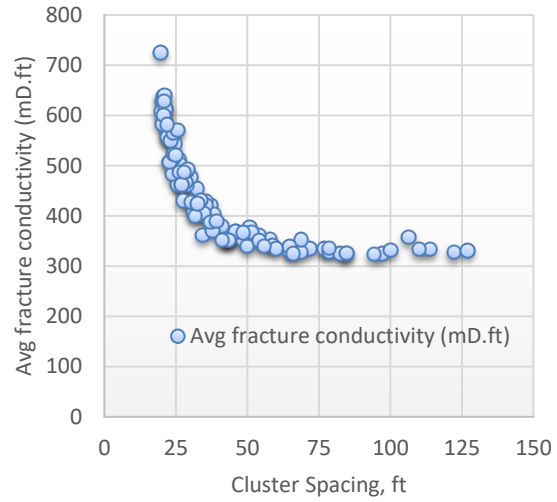


Fig. 23—Average fracture conductivity with cluster spacing.

Number of Clusters per Stage

While keeping everything else constant to the base scenario, the number of clusters per stage was varied from 3 to 7. It is observed that as we increase the clusters/stage, the fracture length drops since the fluid volume per cluster has decreased (**Fig. 24**). The average net pressure (**Fig. 25**) shows a minor ramp up as the number of cluster increases. Other parameters such as surface area, fracture height, fracture conductivity, and fracture width do not show significant variations (**Figs. 26–29**).

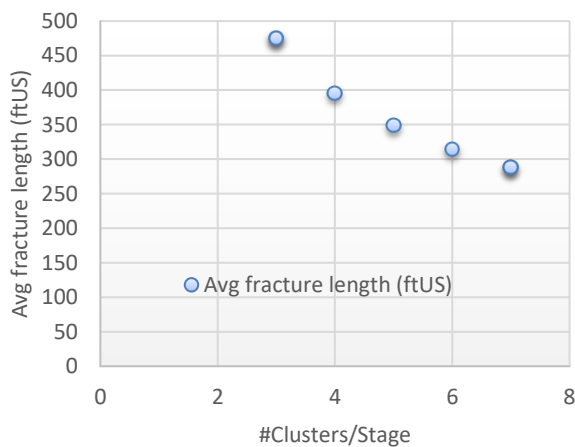


Fig. 24—Average fracture length with number of clusters/stage.

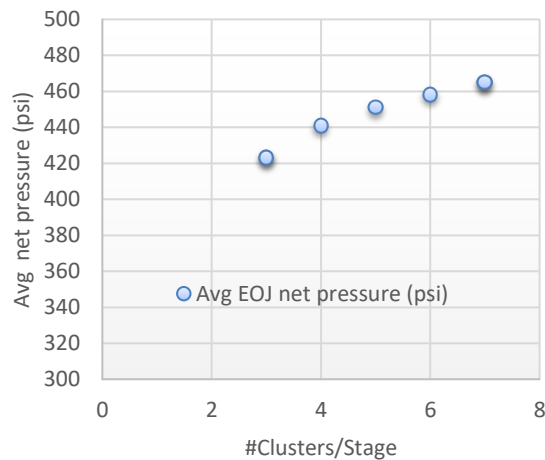


Fig. 25—Average net pressure with number of clusters/stage.

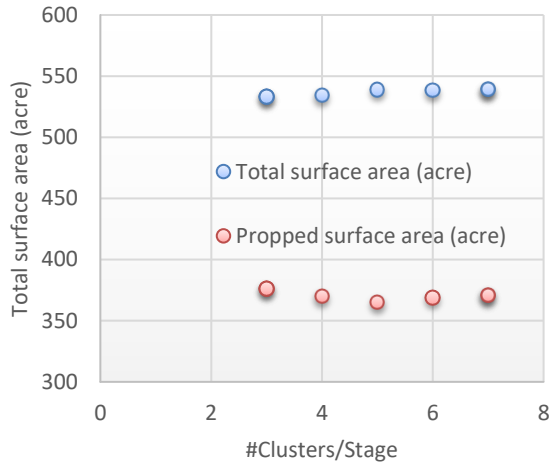


Fig. 26—Total surface area with number of clusters/stage.

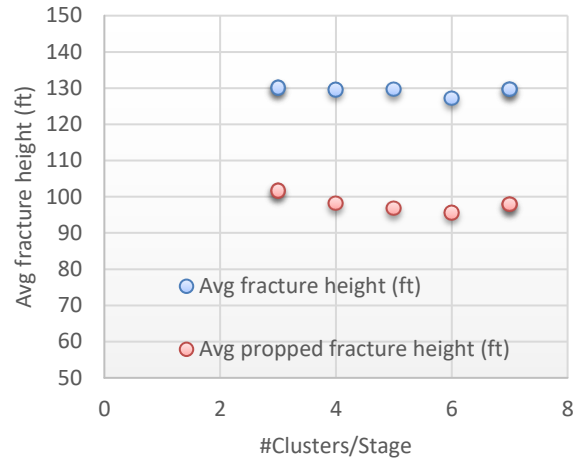


Fig. 27—Average fracture height with number of clusters/stage.

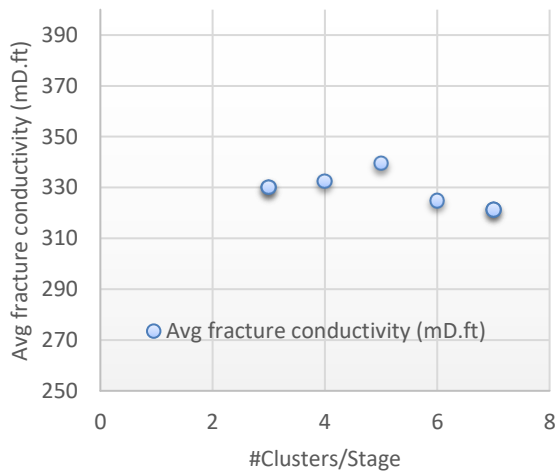


Fig. 28—Average fracture conductivity with number of clusters/stage.

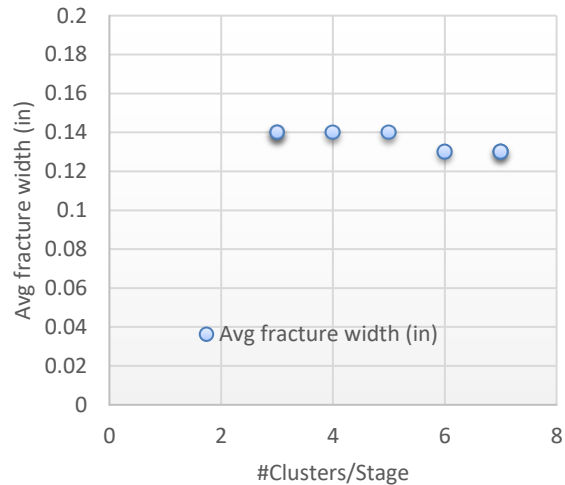


Fig. 29—Average fracture width with number of clusters/stage.

Multiwell Scenario

The single-well optimum completion solution may not fit for the multiple-well scenario. The well-to-well interaction during stimulation as well as production must be accounted for to drive the completion and well-spacing decisions given the fact that the horizontal wells would strongly interact with each other when the treatment designs are pumped with larger volumes or at a different cluster spacing completion design. Furthermore, the sequence of stimulation in a multiple-well scenario plays a critical role in impacting the fracture geometry. Pankaj et al. (2016) studied the effect of zipper fracturing in the Wolfcamp and saw mixed results for the benefits of zipper fracturing on different well pads. Therefore, the well spacing optimization is fundamentally tied together with the well completion optimization.

Well Spacing

Various well spacing scenarios are tested for the sensitivity of well spacing (**Fig. 30**).

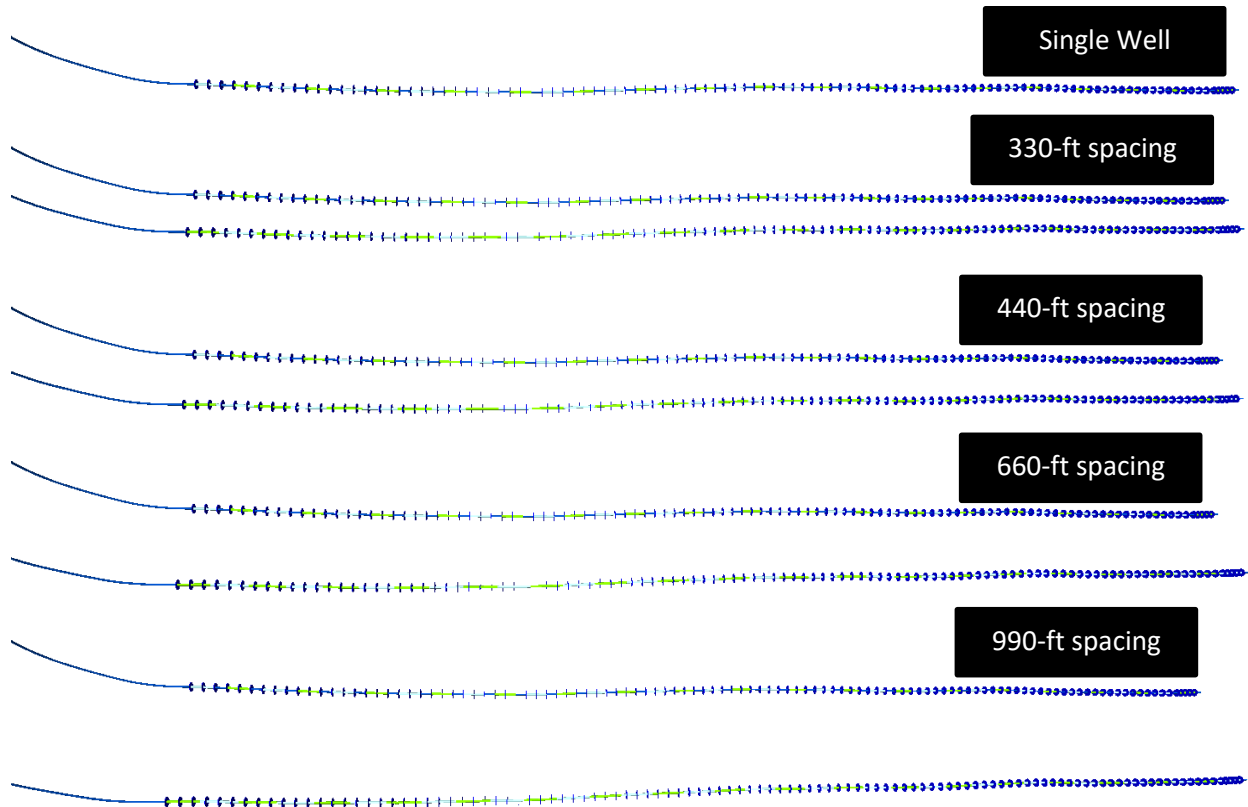


Fig. 30—Different well-spacing scenarios.

When multiple wells are considered in the sensitivity analysis, the trend of the six parameters would stay similar to the observation we made with the single-well sensitivity analysis if the zipper sequencing is not being considered and the wells are treated standalone and having no stress shadow influence from the offset wells. However, when it comes to production, the wells that are close will compete for the same rock volume. There would be production interference on the closely spaced wellbores. It is seen that there is no production interference at the 660-ft well spacing when considering 2-year cumulative production (**Fig. 31**). However, if with tighter well spacing, the production interference significantly increases to ~8% with 440-ft spacing and 18% with 330-ft well spacing (**Fig. 32**). Therefore, the operator may easily run economic analysis to decide whether they can place twice as many wells in the section with 330-ft spacing and compromise with the 18% production drop.

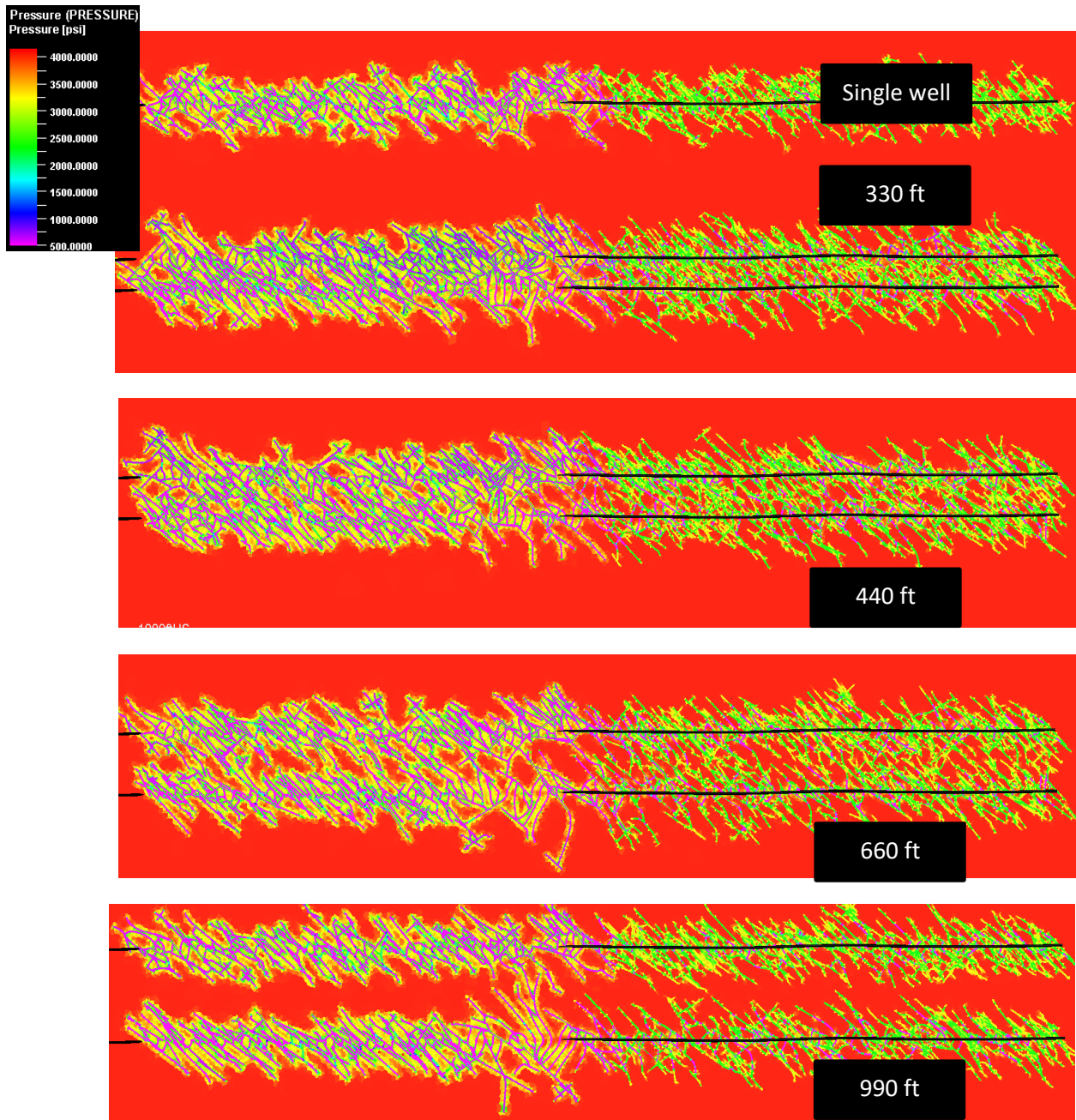


Fig. 31—Pressure depletion pattern for single well and two wells at 330-ft, 440-ft, and 990-ft well spacing.

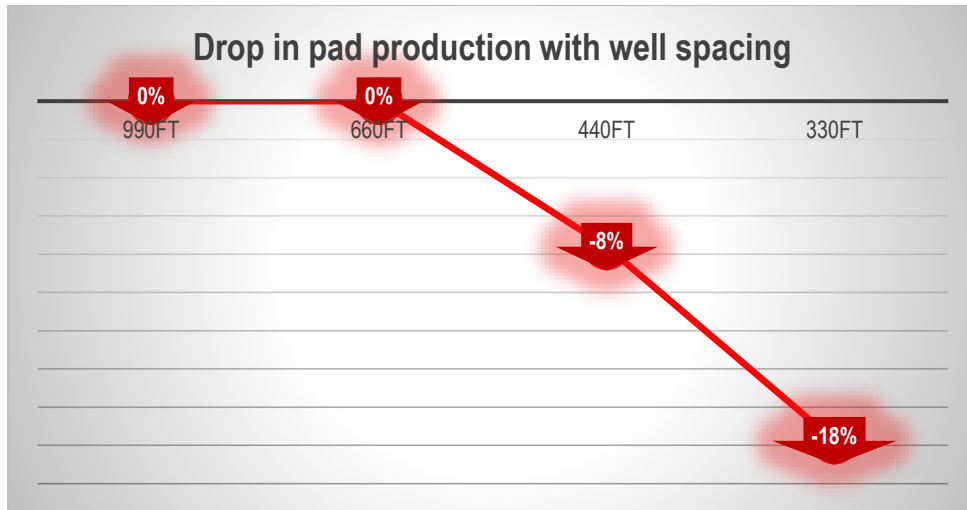


Fig. 32—Sequential production drop when the two wells are spaced closer.

Zipper Fracturing Sequence

Zipper fracturing is an operational technique to complete and stimulate fracturing stages in the wells one after the other as shown in Fig. 33. Fig. 34 shows the configuration of the four wells in the well pad. Two of them are completed in the Upper Wolfcamp and other two are completed in the middle Wolfcamp shale reservoirs. The zipper sequence involves and up to bottom and then again up to bottom sequence, as shown in the schematic in Fig. 34.

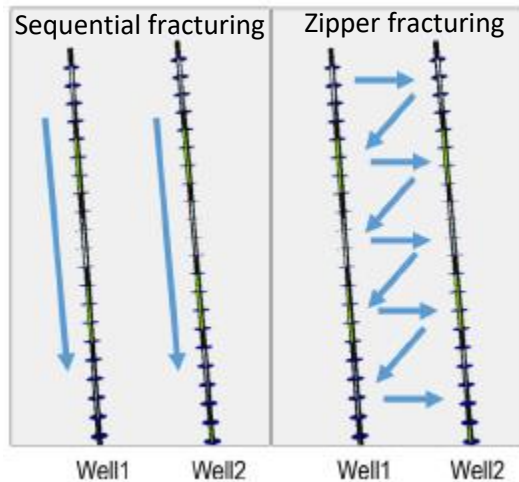


Fig. 33— Sequential fracturing sequence (fracturing well 1 toe-to-heel and then fracturing well 2, versus zipper fracturing sequence (Qiu et al. 2015).

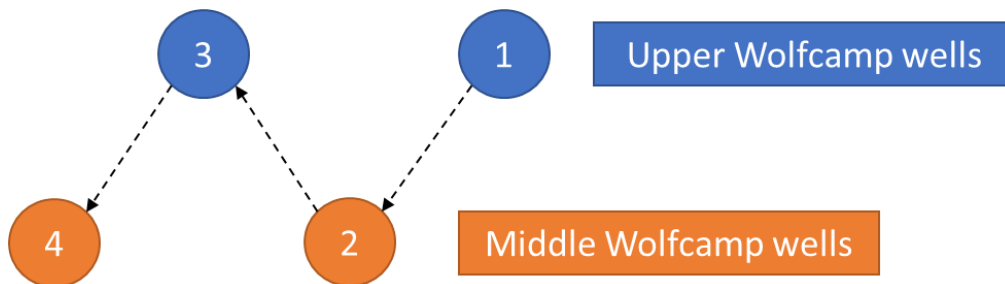


Fig. 34—Schematic for zipper stimulation of wells in Upper and Middle Wolfcamp wells together, number represents the order.

To evaluate the impact of zipper stimulation on the wells, a comparison was made of the zipper stimulation case and the non-zipper sequential stimulation case where the hydraulic fractures in the four wells do not have any stress shadow interference, as if they were treated one after the other.

The total surface area of hydraulic fracture represents the combined effect of all the four wells together. The total surface area as seen in **Fig. 35** does not have a large variation between zippered and sequenced cases until the approximately 2,400-lbm/ft design. As the hydraulic fracture footprint grows larger with bigger treatment sizes (beyond 2,400 lbm/ft), the stress shadow increasingly impacts the hydraulic fracture front propagation and hence the zippered treatment strategy shows reduced surface area when compared to the sequenced stimulation cases.

Interestingly, the zippered treatment has a pronounced impact on the propped surface area (**Fig. 36**). The stress shadow makes the proppant transport in the fractures more difficult as the geomechanical property changes with the evolving fracture footprint constricting some of the fracture branches. However, the propped surface area does not significantly change over the variation of the proppant loading. It shows some maximum surface area at approximately 2,400 lbm/ft and beyond which there is not much added value in increasing the proppant loading.

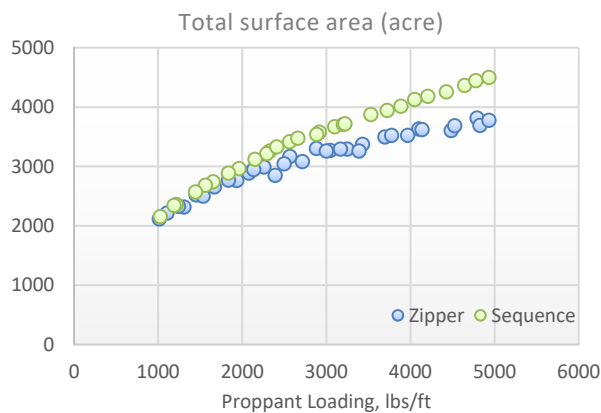


Fig. 35—Total surface area with proppant loading comparison of zippered and sequenced treatments.

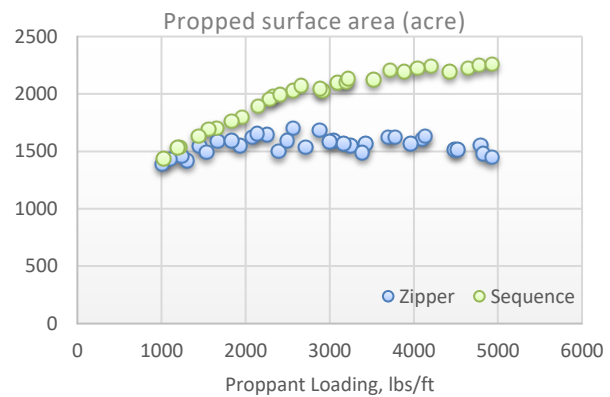


Fig. 36—Propped surface area with proppant loading comparison of zippered and sequenced treatments.

Although higher proppant loading in the fracturing treatment may hurt the economics of the treatment, it also seems to hurt the propped geometry and fracture lengths beyond a certain level. As we try to pump more sand in the created fracture volume, the fracture volume starts to balloon instead of lengthen. The net pressure being created in these fractures starts to build up rapidly when a high volume of sand is being pumped. The net pressure in the rock and the fracture width deformation impacts the intensity of stress shadow. Therefore, at higher proppant loading, the stress shadow increases, which makes the propagation of the hydraulic fracture originating from the offset well even more difficult than the in-situ state of rock. Therefore, beyond an optimum amount of proppant loading, which seems to be approximately 2,400 lbm/ft. from the fracture geometry perspective in these wells, there is reduced benefit.

The length of the fractures also shows the trend that the stress shadow makes when wells oppose each other to reduce the fracture length; the pumped fluid volume increases the fracture height and increases the fracture width instead. Thus, we see that the net pressure inside the fracture increases with amount of proppant loading in a zippered treatment (**Fig. 37**), and the fracture height increases (**Fig. 38**) along with fracture width (**Fig. 39**) and the resulting fracture conductivity (**Fig. 40**).

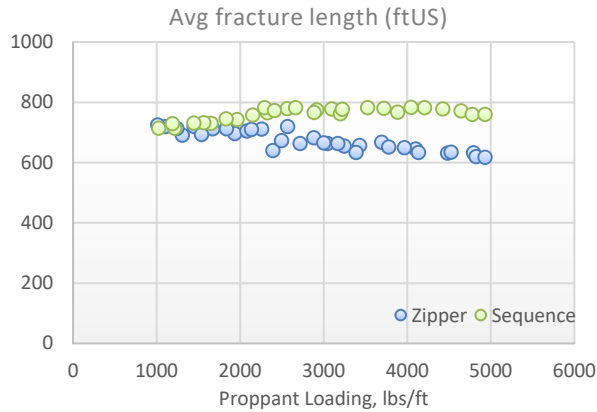


Fig. 37—Average fracture length with proppant loading comparison of zippered and sequenced treatments.

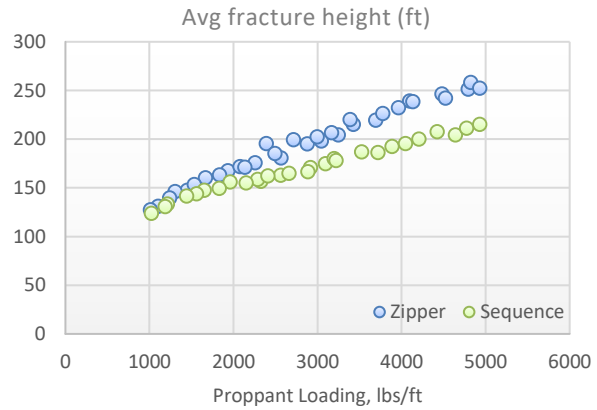


Fig. 38—Average fracture height with proppant loading comparison of zippered and sequenced treatments.

Because of the higher stress shadow effect, the zipper fractures tend to build slightly higher net pressures in the fractures compared to sequenced stimulation operations (Fig. 41).

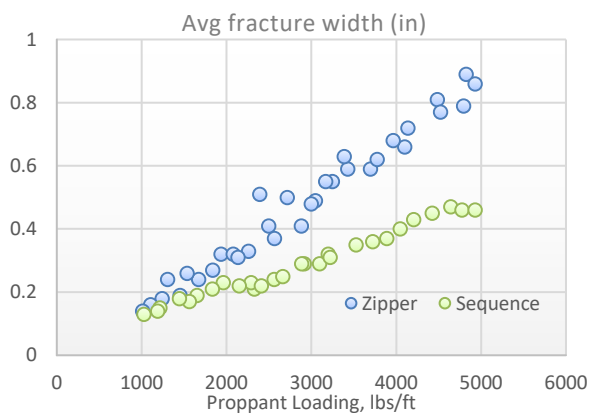


Fig. 39—Average fracture width with proppant loading comparison of zippered and sequenced treatments.

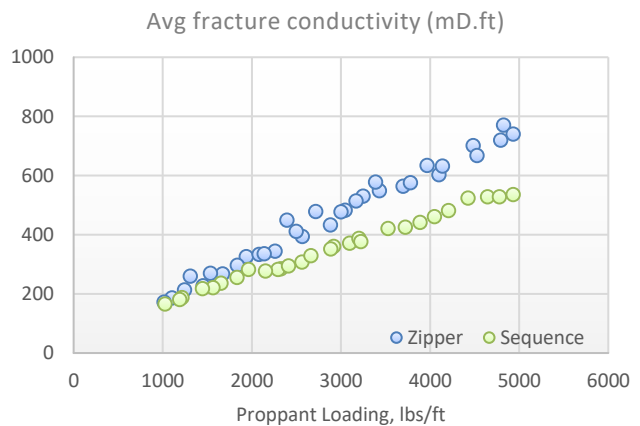


Fig. 40—Average fracture conductivity with proppant loading comparison of zippered and sequenced treatments.

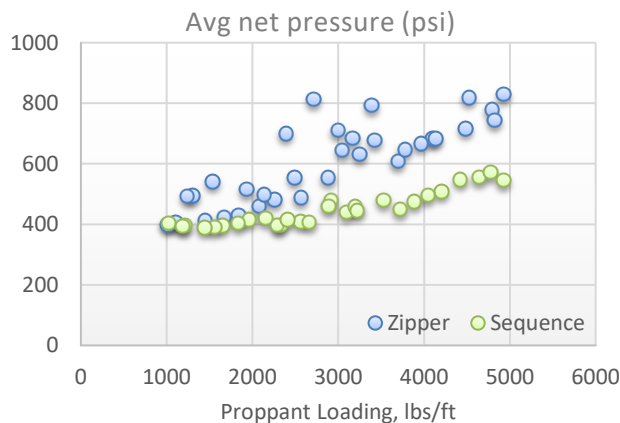


Fig. 41—Average fracture net pressure with proppant loading comparison of zippered and sequenced treatments.

Spacing sensitivity was run on the two Upper Wolfcamp wells for 300 ft to 1,200 ft. As seen from the result represented in **Fig. 42** the total fracture surface area for the two wells plateaus at approximately 660 ft. Similarly, the trend of the net pressures (**Fig. 43**) shows no significant change beyond 660 ft. This suggests that hydraulic fracture interference and stress shadow influence at well spacing above 660 ft starts to decay considerably and the fractures would not be competing with one another significantly. Therefore, from the sensitivity runs, the optimal well spacing for considering the current base completion design is approximately 660 ft.

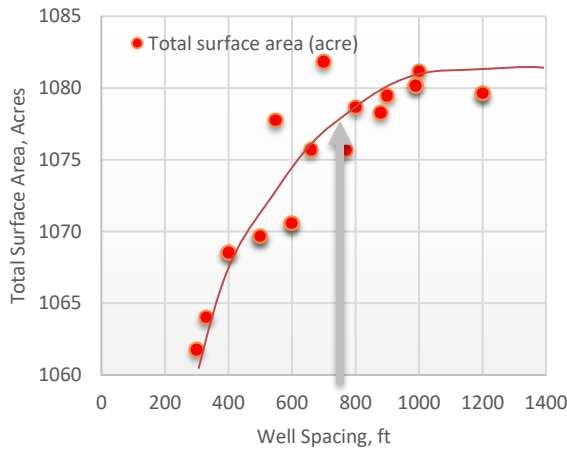


Fig. 42—Total surface area variation with well spacing.

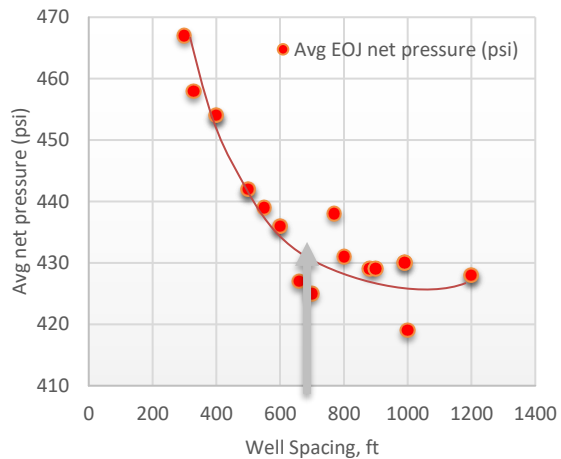


Fig. 43—Average net pressure variation with well spacing.

Impact of Timing of the Child Wells

Several papers have discussed the effect of the parent well-child wells relationship on a well’s productivity (Morales et al. 2016; Marongiu-Porcu et al. 2015; Pankaj et al. 2016 and Pankaj and Shukla (2018)). However, very limited research has been done on understanding the completion optimization and trends for fracture design for completing the child well.

Fig. 44 to **Fig. 46** represents the use of the parent-child well interference workflows, as used in the studies mentioned above, to determine the effect of wellbore depletion on geomechanical properties such as stress magnitude and direction change over a period of time. This change in the geomechanical properties have significant impact on the child well’s hydraulic fracture propagation and hence productivity.

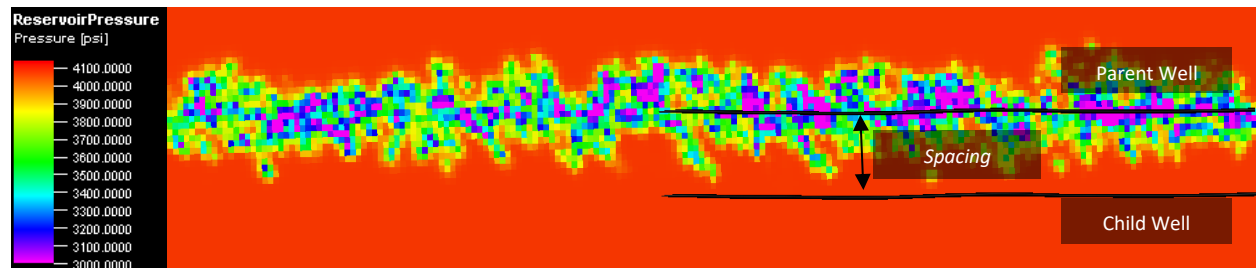


Fig. 44—Reservoir pressure depletion around the parent wellbore after 2 years of production.

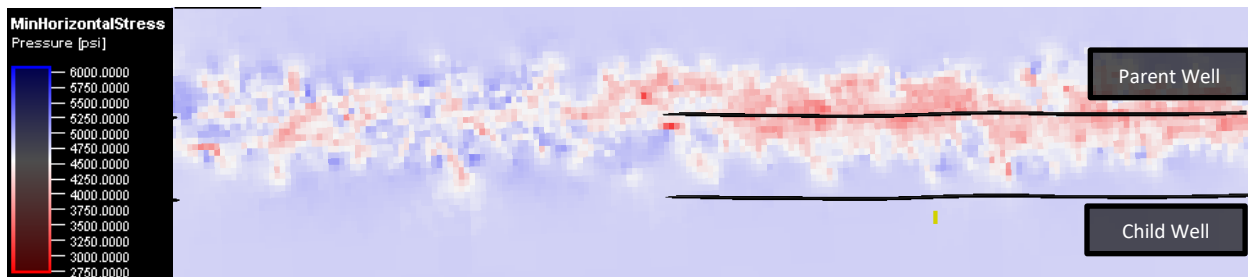


Fig. 45—Minimum horizontal stress change around the parent wellbore calculated through finite element simulation.

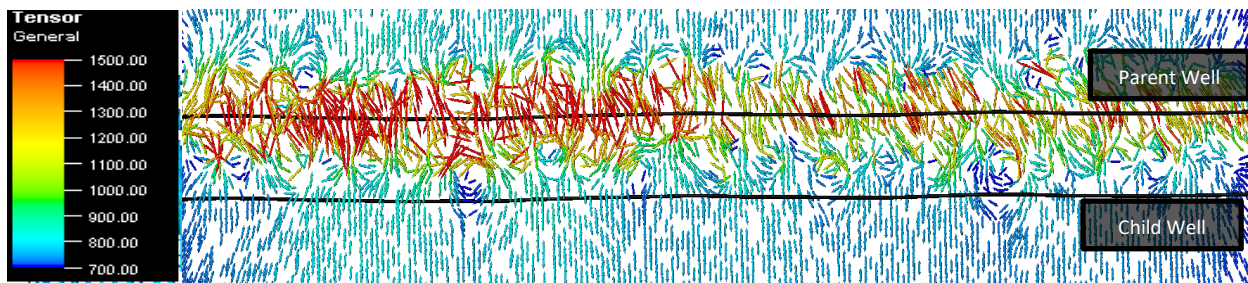


Fig. 46—Maximum horizontal stress direction around the parent wellbore calculated through finite element simulation.

As the stresses reorient near the parent wellbore due to the production through the hydraulic fracture system around the parent wellbore, the stress magnitudes and maximum horizontal stresses change significantly from the original in-situ conditions. If the child wellbore is spaced closely, there is risk of generating considerable number of fracture hits from the child well. Miller et al. (2016) showed that many wells in various basins have been impacted negatively by parent-child hydraulic fracture interactions.

In this study, the child wells were put on completion after 2 years of projection from the parent wellbore. As a result, when the wells are placed at 440 ft and closer, the chances of fracture hits are high. This would impact both parent and child well productivity. Marongiu-Porcu et al. (2015) performed a similar study for Eagle Ford and determined an optimal child well spacing of 600 ft through manual sensitivity. In this study, similarly to the modeling results, it is seen that when the child well is placed 660 ft from the parent wellbore, the child well's hydraulic fractures have minimal or no fracture hit to the parent wellbore (**Fig. 47**). However, when the child wells are 440 ft from the parent wellbore, fracture hits are observed, and a 15% drop in production at 1 year is observed from the parent and child well combination compared to the 660-ft well spacing (**Fig. 48**). Therefore, from a spacing perspective, the child wells must not be placed closer than 660 ft from the parent well in this well pad. Increasing the well spacing beyond 660 ft would, on one hand, avoid any negative impacts due to fracture hits, but, on the other hand, would create upswept regions of the reservoir leading to poor recovery from the pad.

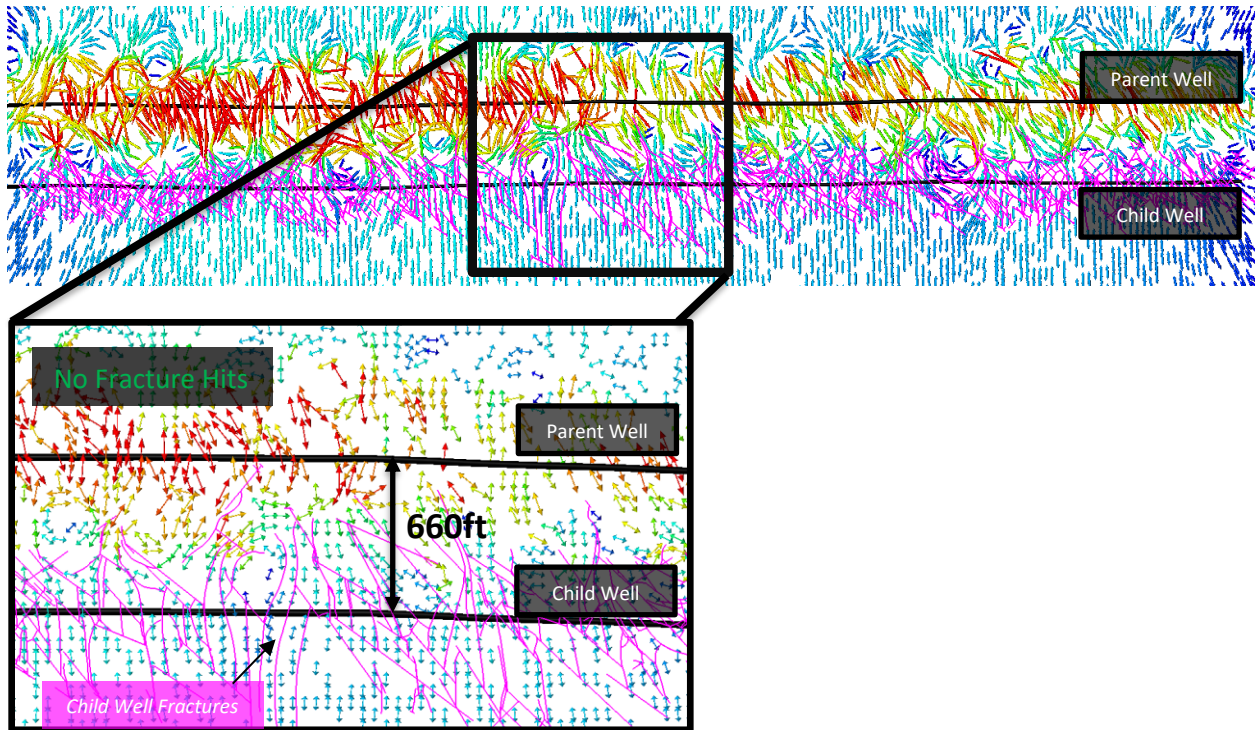


Fig. 47—Child well at 440-ft well spacing shows strong fracture hits from the child well to the parent well.

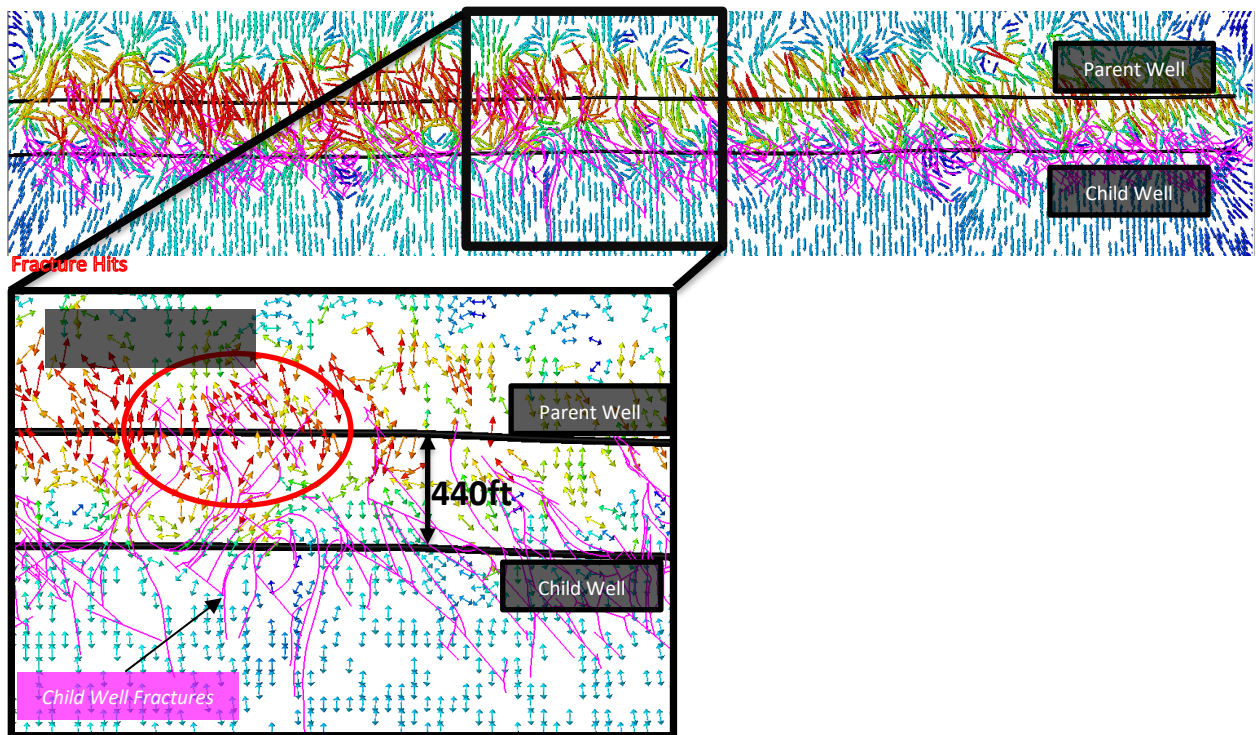


Fig. 48—Child well at 660-ft well spacing shows no fracture hits from the child well to the parent well.

As the stresses reorient near the parent wellbore due to the production through the hydraulic fracture system around the parent wellbore, the stress magnitudes and maximum horizontal stresses change significantly from the original in-situ conditions. If the child wellbore is spaced closely, there is risk of generating considerable number of fracture hits from the child well. Miller et al. (2016) showed that many wells in various basins have been impacted negatively by parent-child hydraulic fracture interactions.

In this study, the child wells were put on completion after 2 years of production from the parent wellbore. As a result, when the wells are placed at 440 ft and closer, the chances of fracture hits are high. This would impact both parent and child well productivity. Marongiu-Porcu et al. (2015) performed a similar study for Eagle Ford and determined an optimal child well spacing of 600 ft through manual sensitivity. In this study, similarly to the modeling results, it is seen that when the child well is placed 660 ft from the parent wellbore, the child well's hydraulic fractures have minimal or no fracture hit to the parent wellbore. However, when the child wells are 440 ft from the parent wellbore, fracture hits are observed, and a 15% drop in production at 1 year is observed from the parent and child well combination compared to the 660-ft well spacing. Therefore, from a spacing perspective, the child wells must not be closer than 660 ft from the parent well in this well pad. Increasing the well spacing beyond 660 ft would, on one hand, avoid any negative impacts due to fracture hits, but, on the other hand, would create upswept regions of the reservoir leading to poor recovery from the pad.

Multiple sensitivity runs were made on the cloud-based parallel computing resource was made to determine if there is any different trend in the fracture geometry of the child wells from that of the parent wellbore.

Because the mass of fluid and proppants is same in the test for the child well, the surface area is very comparable (**Fig. 49**) to that of the parent wellbore. The orientation may change due to the stress reversal, but the surface area generated is not expected to significantly change for the hydraulic fracture geometry. The net pressures in the child are much higher (**Fig. 50**) because the hydraulic fracture now must overcome stronger anisotropy in the formation compared to the parent well.

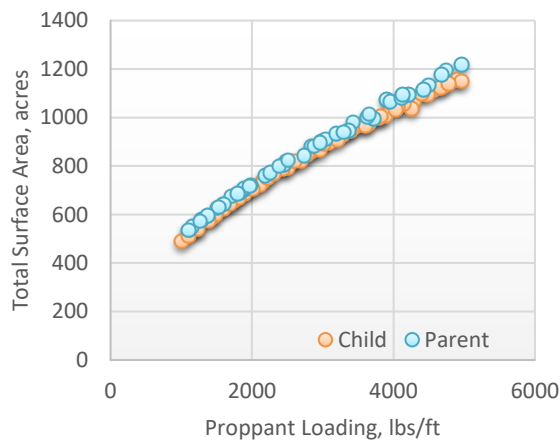


Fig. 49: Surface area with proppant loading

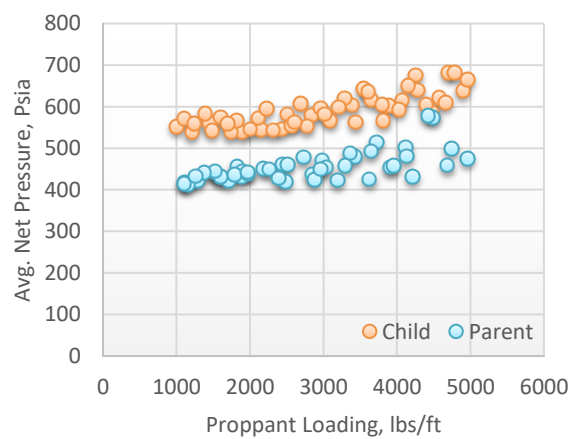


Fig. 50: Avg net pressure with proppant loading

The fracture height (**Fig. 51**) and width (**Fig. 52**) do not significantly change on the child wells.

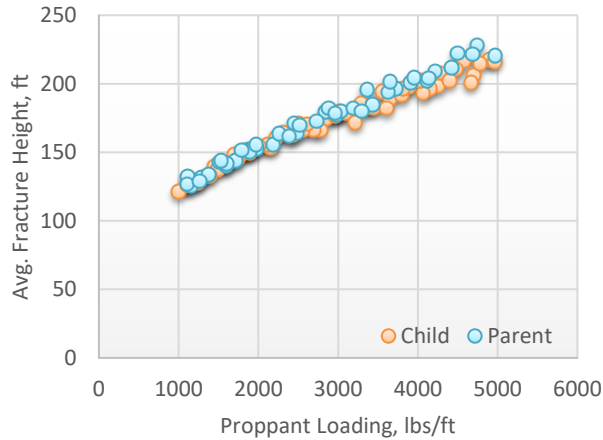


Fig. 51—Average fracture height with proppant loading.

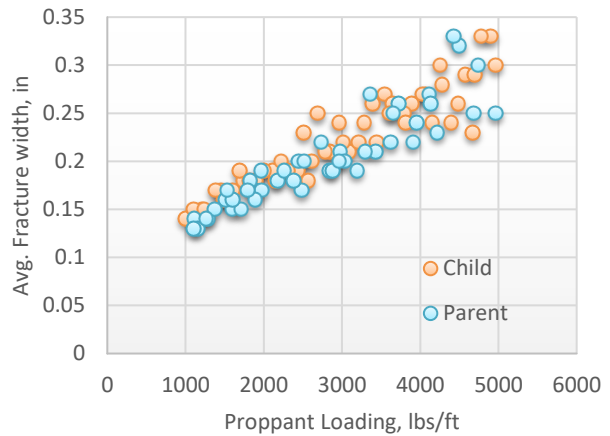


Fig. 52—Average fracture width with proppant loading.

Due to stronger stress cage around the depleted area, the fracture length may drop by 5 to 10% (Fig. 53). Some fracture lengths may be longer due to the pressure sink created in the parent well due to production depletion, but others may show the curving of the fracture due to the change in the stress angle across the fringes of hydraulic fracture geometry of the parent wellbore.

The fracture conductivity is found to be very similar and comparable to that of the parent wellbore (Fig. 54).

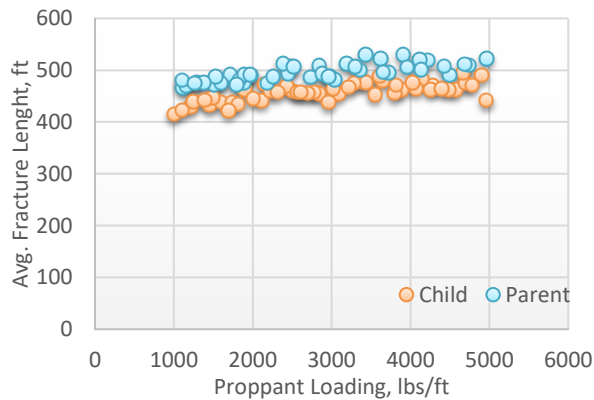


Fig. 53—Average fracture length with proppant loading.

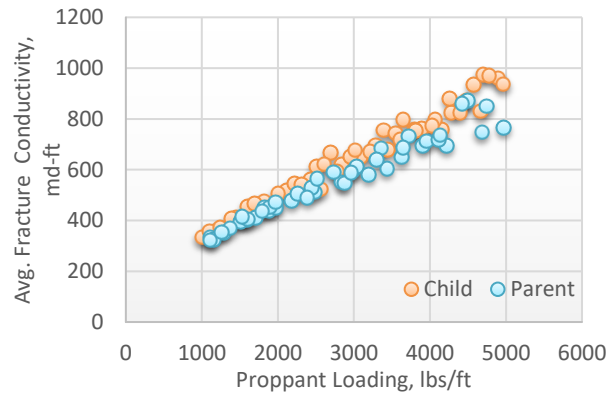


Fig. 54—Average fracture conductivity with proppant loading.

Cluster Spacing Sensitivity for Child Wells

The trends for the parameters such as surface area (Fig. 55) fracture height (Fig.57) analyzed for various cluster spacing on the child wells is similar to those of the parent well sensitivity. However, the net pressure (Fig. 56), average fracture width (Fig. 58), and average fracture conductivity (Fig. 60) are slightly higher whereas the average fracture lengths (Fig. 59) are marginally lower than for the parent well.

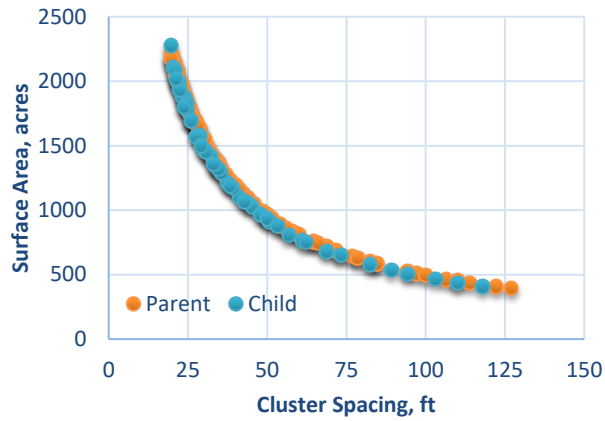


Fig. 55—Surface area with proppant loading.

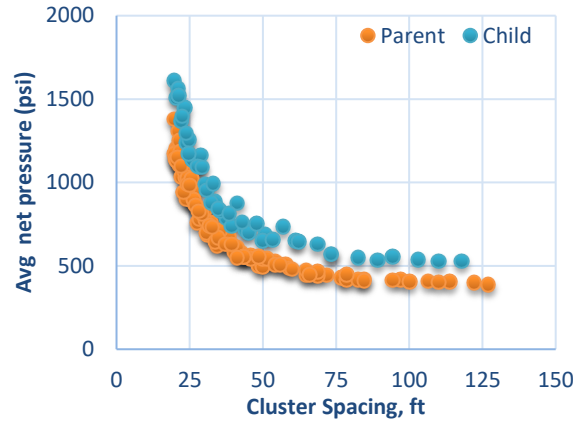


Fig. 56—Average net pressure with proppant loading.

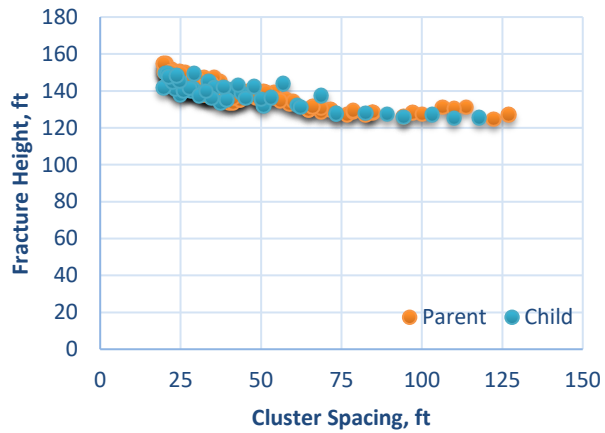


Fig. 57—Average fracture height with cluster spacing

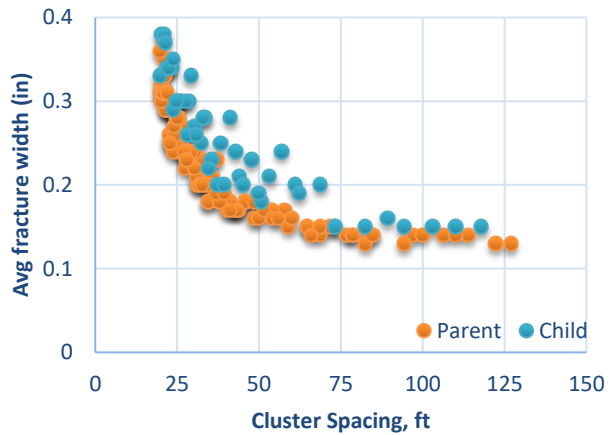


Fig. 58—Average fracture width with cluster spacing.

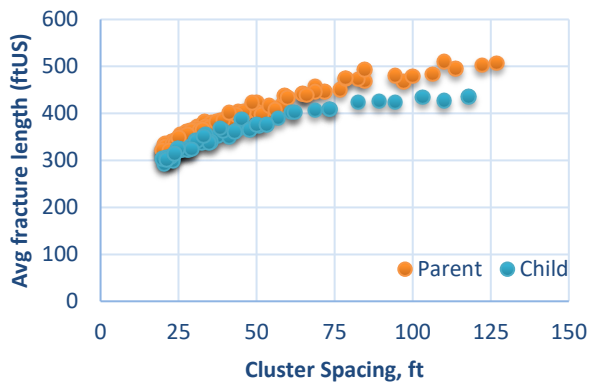


Fig. 59—Average fracture length with cluster spacing.

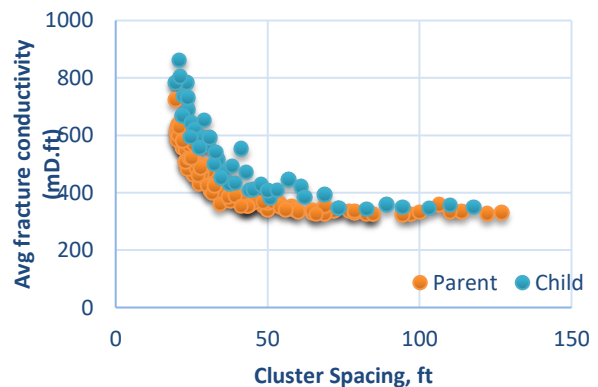


Fig. 60—Average fracture conductivity with cluster spacing.

Discussion

The production enhancement from unconventional reservoirs is extremely challenging because it requires mapping the heterogeneity in the reservoir and characterizing the reservoir quality and placing effective completions in the wellbore. Parallel computing and modeling improves the quality of results because larger number of variable samples can be studied in a short period of time. The wide range of sensitivity in the modeling space allows operators to identify the appropriate direction for completion optimization on the wellsite. This is cheaper than expensive pilot tests and it provides greater confidence in treatment execution, booking reserves, and economic evaluation of the unconventional asset.

In this study, parameters found to have greater impact on productivity were well spacing, cluster spacing, and proppant loading. The production simulation using a numerical simulator coupled to the fracture simulator was also run in the cloud (Fig. 61 and Fig 62).

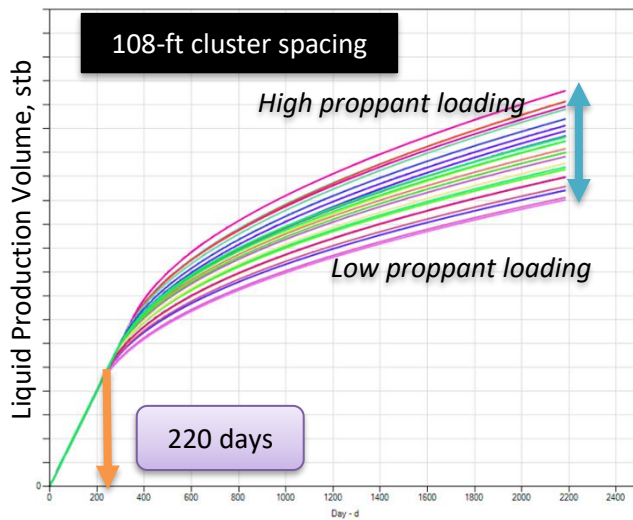


Fig. 61—Production response to various proppant loading at 108-ft cluster spacing.

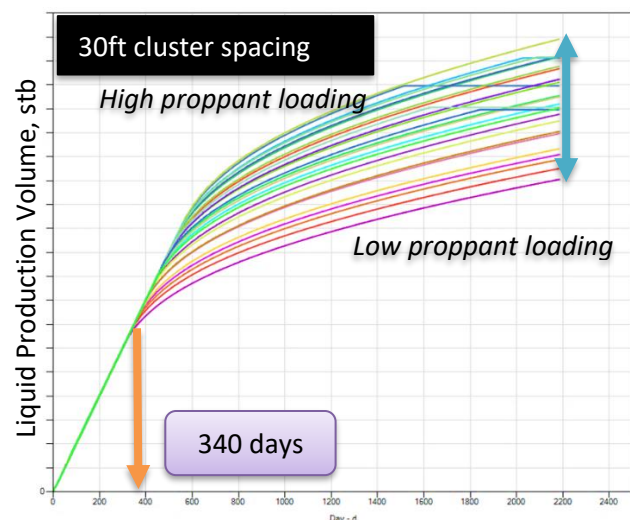


Fig. 62—Production response to various proppant loading at 30-ft cluster spacing.

The Fig. 61 and Fig. 62 shows the production cumulative trend with time (plotted for 6 years) was computed for various proppant loading cases. In general, lower production cumulative at the end of 6 years is expected for the low proppant loading cases and relatively higher production for high proppant loading cases. Two cases of cluster spacings; 108-ft. and 30-ft. are compared. It is seen that for the first 220 days on the 108 ft cluster spacing, the proppant loading does not make any difference in the cumulative production whereas this trend extends to 340 days for the 30ft cluster spacing scenario. Therefore, the reservoir depletion and lower matrix permeability effect kicks in faster with less number of clusters. It's also seen that the variation of production cumulative at the end of 6 years is wider in the 30ft cluster spacing than the 108-ft. cluster spacing. Therefore, increasing the proppant loading has lesser impact on the production in larger cluster spacing than in the tighter spacing and hence it becomes more important to pay attention on pump schedules and treatment designs in a smaller cluster spacing completion to have long term EUR improvement.

Other treating condition and variables such as pump rate, proppant type also shows variability in results and can be sensitized to study the impact (Fig.63 and Fig. 64). Fig. 63 compares various proppant types such as 40/70, 30/50, 20/40 sand at 80% proportion of the job mixed with 100mesh at 20% proportion of the fracturing treatment. Fig. 64 shows the impact of pump rate in generating surface area under various cluster spacing scenarios.

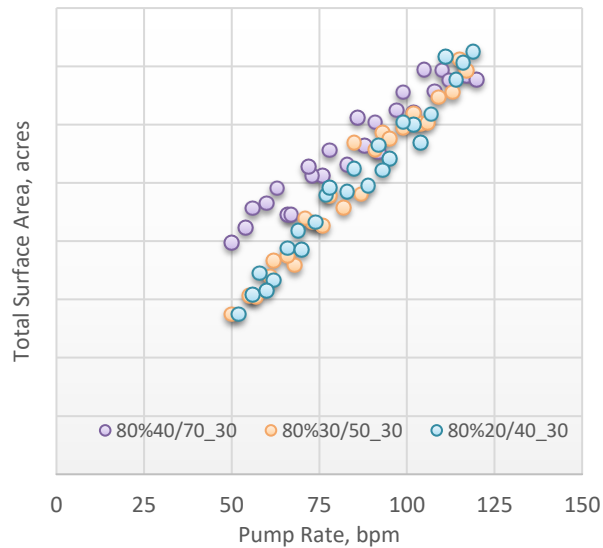


Fig. 63—Total surface area variation with pump rate on different proppants.

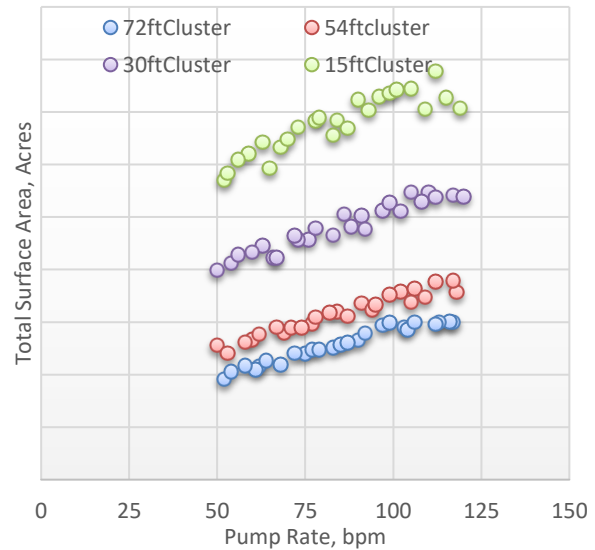


Fig. 64—Total surface area variation with pump rate on cluster spacing.

In the study presented in this paper, over 500 sensitivity cases were run within a week. The same 500 cases would have possibly taken over a few months if they were run manually. Mapping the fracture geometry parameters from these sensitivity cases as trends can provide great insights for determining well completion and well spacing design.

We can use these sensitivities to improve the economics of asset development. As an example, from the sensitivity cases run during the process, **Fig. 65** was created that combines the cluster spacing, as shown in different lines on the chart, and proppant loading on the x-axis as the variables to deduce the production (shown on the y-axis). From a cloud-based sensitivity study on the base model, the trend for the completion variable can be easily derived. Both qualitative and quantitative measures of the impact of any variable can be determined. The sensitivity study presented in Fig. 63 shows that if the operator wants to improve the productivity by 50% on the existing completion plan of 1,800 lbm/ft-treatment design and 108-ft cluster spacing, then 62% extra proppant must be pumped (i.e., approximately 3,000 lbm/ft). However, the same production can be achieved by reducing the cluster spacing to 30 ft and maintaining the treatment design at 1,800 lbm/ft. Economic analysis on both the scenarios would most likely result in bigger cost savings by only considering the change in the completion's cluster spacing. Therefore, having wider understanding of the impact of different completion variables can save considerable cost and provide an efficient and effective design to the operators.

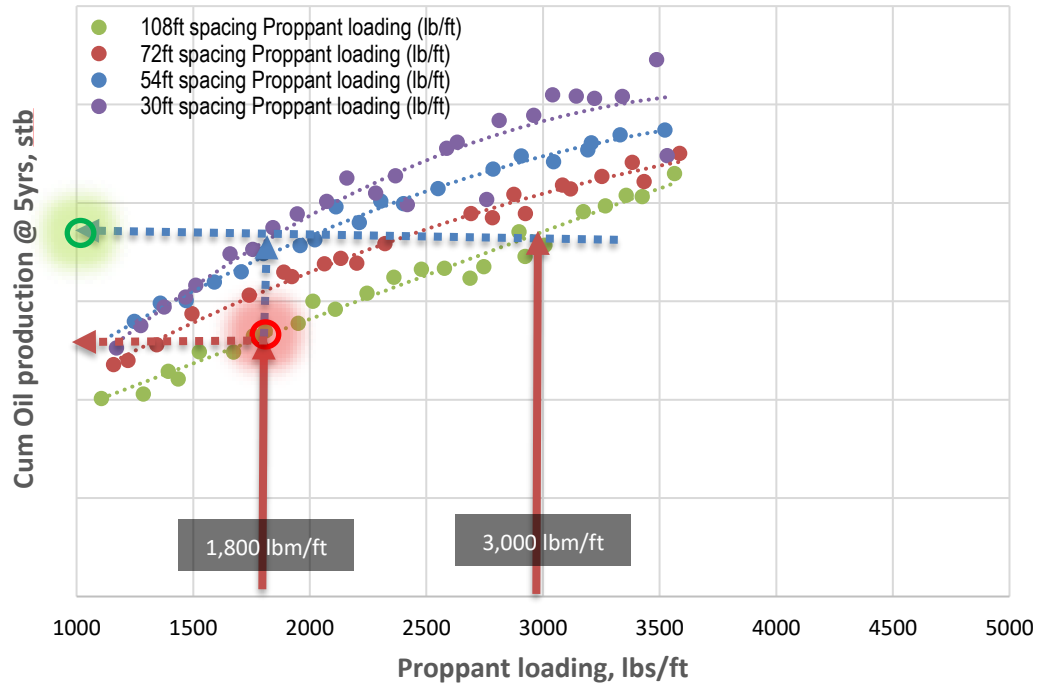


Fig. 65—Oil production response to various cluster spacing and proppant loading.

Conclusions

The well completion optimization process is not merely a matter of looking at one well / stage in singularity but requires the broader consideration of the other wells in the pad. An optimized completion on one stage/ well may not suit all the wells. Paying attention to the well interaction, interference, and recovery is crucial to improve the economics of asset development. Well completion specifics such as pounds per foot of the fracture treatment design, well cluster spacing, timing of fracturing, and sequence of fracturing are critical elements in defining the fracture geometry response and hence the resulting production. Specific learning from cloud-based multivariate analysis in the Wolfcamp formation are as follows:

1. Hundreds of simulations of fracture design are required to understand the trend of hydraulic fracture geometry and productivity. This is only practical when the workflow is powered through cloud-based parallel simulations that thread the hydraulic fracture design, fracture gridding for numerical simulation, and numerical simulation for production response in an automated way. A few hundreds of sensitivity cases can be analyzed within a few days instead of the months required when done manually.
2. Calibration of the base model is a prerequisite of any sensitivity analysis. Hydraulic fracture treatment pressure matching and matching the microseismic footprint may provide calibration points for the fracture geometry whereas production history matching allows reducing petrophysical property uncertainties in the geological model.
3. Increasing the pounds-per-foot design to approximately 3,000 lbm/ft may give optimal results from a fracture geometry perspective at the well spacing of 660 ft in the Wolfcamp. Economics must be the next filter criterion considering the well's drilling and completion cost to determine the "economic" optimal configuration,
4. Shorter cluster spacing has the benefit of concentrating the fracture energy in the near-wellbore region and hence more wells can be placed per section. Production increase is expected due to gaining more surface area near the wellbore with a shorter cluster spacing.
5. Increasing the proppant loading beyond 3,000 lbm/ft does not show significant improvement in the fracture geometry and hence productivity.
6. Increasing the number of clusters per stage does not create a material change in fracture geometry and productivity as long as there are sufficient number of entry holes in the wellbore for fracture initiation and propagation. However, the study does not consider localized lateral heterogeneity that can affect effective

breakdown of the clusters. Optimized well completion with perforation placement in similar rock and limited entry design is important consideration as the number of perforations increase.

7. Fracturing on child wells has similar trends to fracturing on the parent well. However, due to the geomechanical property change with the parent well production, the fracture geometry shows considerable difference from the parent well, especially at well spacing less than 660 ft. A production drop of 15% is observed at 1 yr on the parent and child well combination due to overlapping of fracture geometry competing with the same rock and the fracture hits on the parent originating from the child wellbore.
8. Zipper sequenced treatments have resulted in compressing fracture extents horizontally while increasing fracture height due to the stronger stress shadow effect from the fractures. The stress shadow strength increases with longer fracture lengths created at treatment of jobs over 2,400 lbf/ft.

Acknowledgments

I would like to thank Meyer Bengio, Xiaowei Weng, Hitoshi Onda, and Ken Sheldon for providing resources and support during the study and would like to thank Schlumberger for allowing me to publish this work.

References

1. Baumgardner, R.W., Jr., Hamlin, H. S., and Rowe, H. D. 2014, High-Resolution Core Studies of Wolfcamp/Leonard Basinal Facies, Southern Midland Basin, Texas: Search and Discovery Article #10607. http://www.searchanddiscovery.com/documents/2014/10607baumgardner/ndx_baumgardner.pdf (accessed 21 November 2016).
2. Cipolla, C. L., Fitzpatrick, T., Williams, M. J. et al. 2011a. Seismic-to-Simulation for Unconventional Reservoir Development. Presented at the SPE Reservoir Characterisation and Simulation Conference and Exhibition, Abu Dhabi, UAE, 9–11 October. SPE-146876-MS. <https://doi.org/10.2118/146876-MS>.
3. Collins, D. R., Monson, G., Chu, W. et al. 2015. An Integrated Approach to Stimulated Reservoir Interpretations of the Permian Wolfcamp Shale. Presented at the Unconventional Resources Technology Conference, San Antonio, Texas, USA, 20–22 July. URTEC-2154510-MS. <https://doi.org/10.15530/URTEC-2015-2154510>
4. Gaswirth, S. B., Marra, K. R., Lillis, P. G. et al. 2016. Assessment of Undiscovered Continuous Oil Resources in the Wolfcamp Shale of the Midland Basin, Permian Basin Province, Texas, 2016: U.S. Geological Survey Fact Sheet 2016–3092. <https://doi.org/10.3133/fs20163092>.
5. Marongiu-Porcu, M., Lee, D., Shan, D. et al. 2015. Advanced Modeling of Interwell Fracturing Interference: an Eagle Ford Shale Oil Study. Presented at the SPE Annual Technical Conference and Exhibition, Houston, Texas, USA, 28–30 September. SPE-174902-MS. <https://doi.org/10.2118/174902-MS>
6. Peacock, R., Stackhouse, B., and Patel, P. 2018. Proppant Demand Outlook for the Bakken and Permian. Energy Insights by McKinsey. <https://www.mckinseyenergyinsights.com/insights/proppant-demand-outlook-for-the-bakken-and-permian/> (accessed 1 April 2018).
7. Miller, G., Lindsay, G., Baihly, J. 2016. Parent Well Refracturing: Economic Safety Nets in an Uneconomic Market. Presented at the SPE Low Perm Symposium, Denver, Colorado, USA, 5-6 May. SPE-180200-MS. <https://doi.org/10.2118/180200-MS>
8. Mohan, K., Scott, K. D., Monson, G. D. et al. 2013. A Systematic Approach to Understanding Well Performance in Unconventional Reservoirs: A Wolfcamp Case Study. Presented at the Unconventional Resources Technology Conference, Denver, Colorado, USA, 12–14 August. <https://doi.org/10.1190/urtec2013-051>.
9. Morales, A., Zhang, K., Gakhar, K. et al. 2016. Advanced Modeling of Interwell Fracturing Interference: An Eagle Ford Shale Oil Study - Refracturing. Presented at the SPE Hydraulic Fracturing Technology Conference, The Woodlands, Texas, USA, 9–11 February. SPE-179177-MS. <https://doi.org/10.2118/179177-MS>
10. Pankaj, P., Gakhar, K., and Lindsay, G. 2016. When to Refrac? Combination of Reservoir Geomechanics with Fracture Modeling and Reservoir Simulation Holds the Answer. Presented at the SPE Asia Pacific Oil & Gas Conference and Exhibition, Perth, Australia, 25–27 October. SPE-182161-MS. <https://doi.org/10.2118/182161-MS>.
11. Pankaj, P., and Shukla, P. 2018. Application of Refracturing Using Coiled Tubing Opens a New Door of Opportunities for Unconventional Reservoir Stimulation. Presented at the SPE/ICoTA Coiled Tubing and Well Intervention Conference and Exhibition, The Woodlands, Texas, 27–28 March. <https://doi.org/10.2118/189933-MS>

12. Qiu, F., Porcu, M. M., Xu, J. et al. 2015. Simulation Study of Zipper Fracturing Using an Unconventional Fracture Model. Presented at the SPE/CSUR Unconventional Resources Conference, Calgary, Alberta, Canada, 20–22 October. SPE-175980-MS. <https://doi.org/10.2118/175980-MS>
13. Weng et al 2011 Numerical Modeling of Hydraulic Fracturing in Naturally Fractured Formations. Presented at the 45th US Rock Mechanics/Geomechanics Symposium, San Francisco, California USA, 26-29 June.
14. Weng, X. 2014. Modeling of Complex Hydraulic Fractures in Naturally Fractured Formation. *Journal of Unconventional Oil and Gas Resources* **9**: 114–135.